Memoirs of the Faculty of Engineering, Nagoya University
Vol. 40, No. 2 (1988)

CHATTERS OF A WORKPIECE ARISING IN LATHES

HIROSHI OTA, KAZUKI MIZUTANI*,
and TADAO KAWAI

Department of Mechanical Engineering

(Received October 31, 1988)

Abstract

In this paper the authors researched primary and regenerative chatters, especially their transient behavior. To this end, the authors measured the following quantities by use of a computer-aided measuring system: the horizontal and vertical deflections of a workpiece; the horizontal and vertical cutting forces; the depth of cut. Further, the behavior of a generated chip was observed by use of a high-speed camera. Then, the authors found out the relation between a workpiece deflection and cutting forces and compared cutting forces through initial chip generation. These investigations showed the following transient properties of chatter. A small disturbance which is able to occur under any cutting conditions causes a built-up of chatter under a certain cutting condition. The roundness of the cutting edge, a rake angle of tool and the depth of cut have a significant effect on primary chatter.

As a result of this investigation, physical causes of the primary chatter and properties of the dynamic cutting force are revealed.

Contents

* Department of Mechanical Engineering, Mie University

Chapter 1. General Introduction

Since the machine tool was invented, improvements in cutting accuracy and cutting efficiency have been important subjects. In the course of the work on improvements, chatter has been one of the most troublesome problems. Because it interrupted a cutting operation, made bad machined surface, imposed restrictions on the cutting conditions and wore the tool rapidly.

On the study of chatter, following four questions are very important. What phenomenon occurs when chatter takes place? What is the physical cause of chatter? Under what cutting condition does chatter occur? Which factor affects chatter? In short words, the description of chatter and the prediction of the limit of the cutting stability are aims of the study of chatter. R.N. Arnold,[1] R.S. Hahn,[2] S. Doi,[3-9] S. Kato,[10] P. Albrecht[11] and so on described the physical causes of chatter and its properties experimentally. S.A. Tobias,[12] S. Doi,[13] S. Kato,[14-15] H. Ota and K. Kono[16-18] and so on predicted the stability limit theoretically. These works indicated the effects of the static cutting force, cutting conditions and coupling of the system on chatter. However, there lacked the consideration on dynamic cutting force so that the good prediction of the stability limits wasn't achieved.

In this paper, the authors, first, described the transient properties of cutting soon after the cutting operation began by use of a computer-aided measuring system and a high speed camera. Then the authors revealed cutting dynamics and physical causes of chatter. Especially following four matters were investigated.

(1) The confirmation whether the equation of motion being the base of the prediction of stability limits expressed chatter sufficiently.
(2) The relation between the occurrence of chatter and the dynamics of cutting soon after the cutting operation began.
(3) The effects of the configuration of a tool, i.e., roundness of the cutting edge or a rake angle, on the static or the dynamic cutting force.
(4) The relation between the static or the dynamic cutting force and the physical cause of chatter.

Chapter 2. On the Occurrence of Regenerative Chatter Vibration[21,22]

2. 1. Introduction

In lathe operations, when a regenerative chatter vibration is caused by a small disturbance, it is impossible to continue cutting operation. Hence, for a long time, many investigators have researched the stability limit of regenerative chatter. Doi and Kato[13], Ota and Kono[17,18] determined the stability limit using their experimental results, where the fluctuation of cutting forces lagged behind the depth variations. Tobias and Fishwick[12] determined it by considering the penetration effect. Recently some reports concerning the regenerative effect on a chatter vibration were published. Kondo et al.[19] showed that the multiple regenerative effect suppressed chatter vibration when an amplitude of a workpiece vibration was so large that the workpiece partly left a tool. Also, Kaneko et al.[20] proposed differential equations of motion with two degrees of freedom after investigating experimental data of the cutting force and the workpiece deflection.

However, it has not yet been determined whether a small waviness with constant amplitude exists or not on a workpiece surface, as suggested by theoretical analysis in the case of the stability limit, and how a large disturbance causes regenerative chatter. With exception of Hahn,[2] nobody investigated how chatter vibration grows under the influence of a regenerative effect because of the many difficulties in measuring cutting forces and workpiece deflections in the initial stage.

One of the purposes of this chapter is to determine the following influences: (1) the influence of a small change of a cutting force on regenerative chatter; (2) the influence of regenerative effect on chatter vibration; (3) and the relation between the cutting force and the workpiece deflection. For this purpose, the authors used a micro-computer. Another purpose is to propose more suitable differential equations of motion. To verify the agreements of the theoretical results with the experimental results the authors compared both results for two different cases: first, where the workpiece suffered a small disturbance of displacement, and second, where the workpiece was disturbed by a hammer blow. The authors measured the characteristics of two components of the cutting force, and numerically solved the differential equations of motion using these experimental values.[21,22]

2. 2. Equations of motion

Here we consider a vibratory system with two degrees of freedom in which the stiffness of a workpiece is considerably lower than that of a tool, and only a workpiece is assumed to deflect. For this system the orthogonal coordinates system O-$\xi\eta$ is not generally considered in accordance with the orthogonal coordinates O-xy. Here, O-$\xi\eta$ consists of two normal coordinates[21,36] of natural vibration and O-xy consists of two rectangular coordinates, horizontal axis x and vertical axis y. Further, the origin O is the

equilibrium point of the workpiece in no operation of cutting.

Now, with regards to the coordinate system O-$\xi\eta$, the authors introduce spring constants k_ξ, k_η and damping coefficients c_ξ, c_η as follows:

$$\left.\begin{aligned} k_\xi &= (1+\Delta_k)k, \quad k_\eta = (1-\Delta_k)k \\ c_\xi &= (1+\Delta_c)c, \quad c_\eta = (1-\Delta_c)c \end{aligned}\right\} \tag{1}$$

where k is the arithmetic mean value of spring constant and c is also the mean value of damping coefficient. With no operation of cutting, the differential equations of motion of the workpiece regarding the coordinate system O-$\xi\eta$, are as follows:

$$\left.\begin{aligned} m\ddot{\xi} + c_\xi\dot{\xi} + k_\xi\xi &= 0 \\ m\ddot{\eta} + c_\eta\dot{\eta} + k_\eta\eta &= 0 \end{aligned}\right\} \tag{2}$$

Eq. (2) is then transformed into the equations expressed in the coordinate system O-xy using Eq. (3).

$$\begin{pmatrix} \xi \\ \eta \end{pmatrix} = \begin{pmatrix} \cos\alpha & \sin\alpha \\ -\sin\alpha & \cos\alpha \end{pmatrix} \begin{pmatrix} x \\ y \end{pmatrix} \tag{3}$$

Further, the horizontal cutting force F_x and the vertical cutting force F_y are added to the right-hand sides of equations of motion regarding with x and y.

Here, the following parameters are introduced; $p=\sqrt{k/m}$, $n=c/(2m)$ and

m: equivalent mass of the workpiece assumed to be concentrated on the A-A plane as shown in Fig. 2. 1(a).

α: angle$\angle$ xOξ between the coordinate axis ξ and the coordinate axis x as shown in Fig. 2. 1(c). Counter-clock-wise direction is taken as positive one.

d_0: constant feed rate (mm/rev)

d: instantaneous depth of cut. General expression is as follows:

$$d = min\ \{d_0 + x(t-T) - x(t),\ 2d_0 + x(t-2T) - x(t),\ \ldots\} \tag{4}$$

where T is the time required for the workpiece to rotate a complete one revolution. However, if d has a negative value in Eq. (4), d is taken as zero.

Finally, using the following dimensionless quantities (5),

$$\left.\begin{aligned} x' &= x/d_0, \quad y' = y/d_0, \quad t' = pt \\ f_x &= F_x/(kd_0), \quad f_y = F_y/(kd_0) \end{aligned}\right\} \tag{5}$$

the authors obtain dimensionless differential equations of motion (6) concerning the coordinate system O-xy. Hereafter, the prime, representing dimensionless quantities, is omitted.

$$\ddot{x}+(2n/p)(1+\Delta_c\cos 2\alpha)\dot{x}$$
$$+(2n/p)\,\Delta_c(\sin 2\alpha)\dot{y}$$
$$+(1+\Delta_k\cos 2\alpha)x+\Delta_k(\sin 2\alpha)y=f_x(d)$$
$$\ddot{y}+(2n/p)\,\Delta_c(\sin 2\alpha)\dot{x}$$
$$+(2n/p)(1-\Delta_c\cos 2\alpha)\dot{y}$$
$$+\Delta_k(\sin 2\alpha)x+(1-\Delta_k\cos 2\alpha)y=f_y(d) \qquad (6)$$

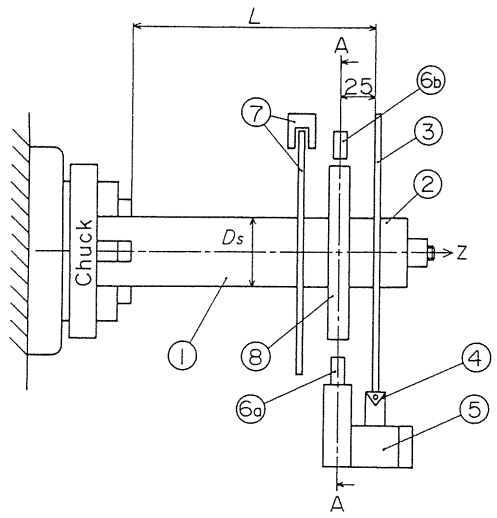

(a) Plane view

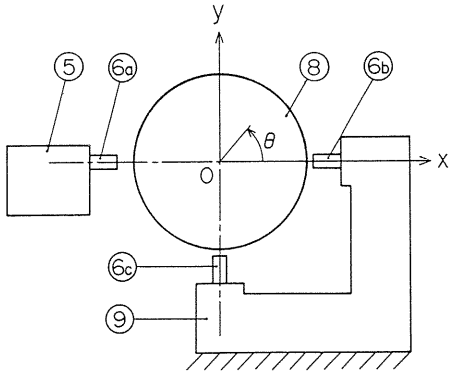

(b) Cross section A-A viewed from z axis

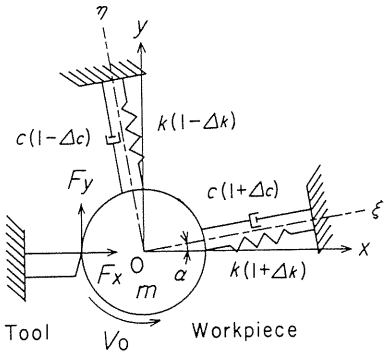

(c) Model of a workpiece with two degrees of freedom

Fig. 2. 1. Experimental apparatus

2. 3. Experimental apparatus and measuring procedure

In experiments, the authors measured the following quantities: both of the horizontal deflection x and the vertical deflection y of a workpiece; a relative displacement between the workpiece and the tool; two components of the cutting force, F_x and F_y; revolution marks of the workpiece. Figs. 2. 1(a), (b) and (c) show the schematic view of the experimental apparatus. A workpiece was cut in the orthogonal cutting condition with the

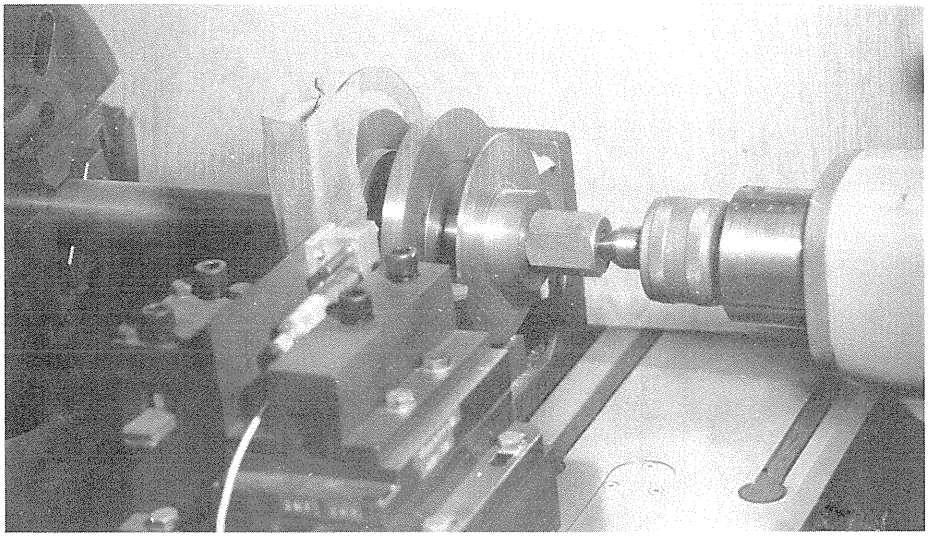

(d) Photograph of the experimental apparatus

Fig. 2. 1. Experimental apparatus (Continued)

Table 2. 1. Vibratory properties of workpiece

Chapter		2	3, 4, 5	5
Diameter of workpiece	Ds (mm)	60	40	40
Length of workpiece	L (mm)	270	300	300
RMS value of natural frequency	$p/(2\pi)$ (Hz)	170	243	111
Spring constant	k (MN/m)	6. 8	11. 6	2. 11
	Δk	−0. 06	−0. 06	−0. 02
Damping coefficient	n/p	0. 073	0. 046	0. 012
	Δc	0. 35	0. 14	0. 70
Equivalent mass	m (kg)	5. 96	4. 96	4. 34
Angle between principal coordinates and generalized ones	α (°)	−10	16	11

Table 2. 2. Configuration of tool

Chapter	2	4, 5	3, 5
Clamp holder	ETFNR2020K33	ETFNR2020K33	EGHR2525M5
Throw away chip	TNPL332 (Cemented carbide)	TNPA332 (Cemented carbide)	EGT5 (Cermet)
Class (JIS)	M20	M20	P20
Back rake angle	−5°	−5°	10°
End relief angle	5°	5°	6°
Side rake angle	5°	5°	0°
Side relief angle	5°	5°	0°
Radius of tool edge	40 μm	36 μm	70 μm

lathe (OKUMA, LS 540×800 type). The steel shaft ① was held by a four-jaw 12 inch chuck at one end in order to reduce the effect of the chuck itself.[23] Further, in the chapters 3, 4 and 5 this shaft is supported by the tailstock at the other end. Table 2. 1 shows its diameter and length adopted in each chapter. By use of holder ②, this shaft carried a workpiece ③ (Brass, JIS H3201 BsP3) of width 2 or 3 mm and of diameter nearly 150 mm. The tool ④ consisted of the clamp holder and a throw-away tip being changed in every cutting operation. Table 2. 2 shows the clamp holder and a throw-away tip adopted in each chapter. The dynamometer ⑤ for measuring two components of the cutting force was a piezo-electric transducer (Kistler, Type 9257A) giving a highly rigid measuring rig with high natural frequency. Three displacement pick-ups ⑥a, ⑥b and ⑥c of eddy current type (AEC-1553T) were used: ⑥a was used for measuring a relative displacement between the tool and the workpiece and to measure a depth of cut; ⑥b was used for the horizontal deflection x; and ⑥c was used for the vertical deflection y. By measuring the revolution marks generated by the photo-interrupter ⑦, the authors controlled and changed the cutting speed continuously by use of a stepless speed changer. These signals were supplied to a data recorder (TEAC, MR-30) and then fed into a micro-computer (North Star Horizon, Black-Box). This computer recorded them during 2. 5 s in digital form at 4000 data points per second per channel. The authors investigated these data by using Nagoya University central computer (FACOM M382). Fig. 2. 2 shows this procedure.

For our purpose, the following special apparatus were equipped.

(a) To measure these data from the start of the cutting operation, the authors installed a trigger pulse generator in the feed device of the lathe.

(b) To detect the instant when a hammer touched the shaft carrying a workpiece, the device to generate a pulse signal at that instant was designed.

(c) For high accuracy, the material ⑧ facing the displacement pick-ups ⑥a, ⑥b, ⑥c was made of brass.

(d) To install a dynamometer and displacement pick-ups on the lathe with high rigidity, the authors used the block ⑨, etc., made of cast iron.

Further, the authors used a high-speed camera (NAC, DF-16C) in the Chapter 3 and 4 to correlate the behavior of a generated chip with quantities measured by the computer-aided system. The authors defined the positive direction of these measured

quantities as follows: upward for a vertical cutting force F_y, to the right for a horizontal cutting force F_x, counter-clockwise for a rotating angle θ (see also the coordinate system O-xy shown in Fig. 2. 1(b)). Cutting conditions were taken as shown in Table 2. 3.

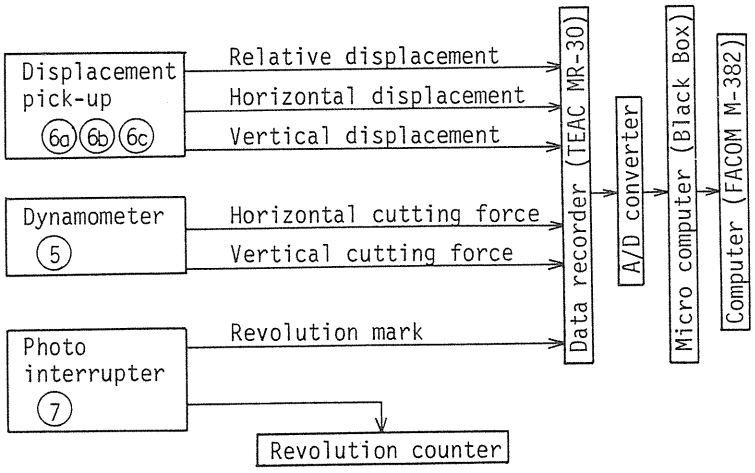

Fig. 2. 2. Block diagram of measuring method

Table 2. 3. Cutting condition

Width b (mm)	Feed d_0 (mm/rev)	Cutting speed V_0 (m/min)
2. 0	0. 05 ~0. 25	100~200
3. 0	0. 025~0. 25	50~200

2. 4. *Experimental Results and Calculated Ones*

2. 4. 1. *Vibratory properties of workpiece*

In preliminary operations without cutting, the authors hit the workpiece with a hammer and measured the natural frequency and damping coefficient of the workpiece. Fig. 2. 3 shows typical wave forms of deflections x and y, where the upper figure shows the wave form derived by a disturbance of ξ-direction and the lower figure by a disturbance of η-direction. Though a small non-linearity of the damping coefficient exists in Fig. 2. 3, the authors neglected this non-linearity and estimated the viscous damping coefficient from a wave form at an amplitude of about 0.05 mm. The spring constant was evaluated by a ratio of a cutting force to the deflection caused by it. The difference Δ_k of the two spring constants, k_ξ and k_η, was in good agreement with the difference calculated from natural frequencies in both ξ and η directions. Table 2. 1 shows these vibratory parameters. Also in this table, vibratory parameters in the Chapters 3, 4 and 5 are given.

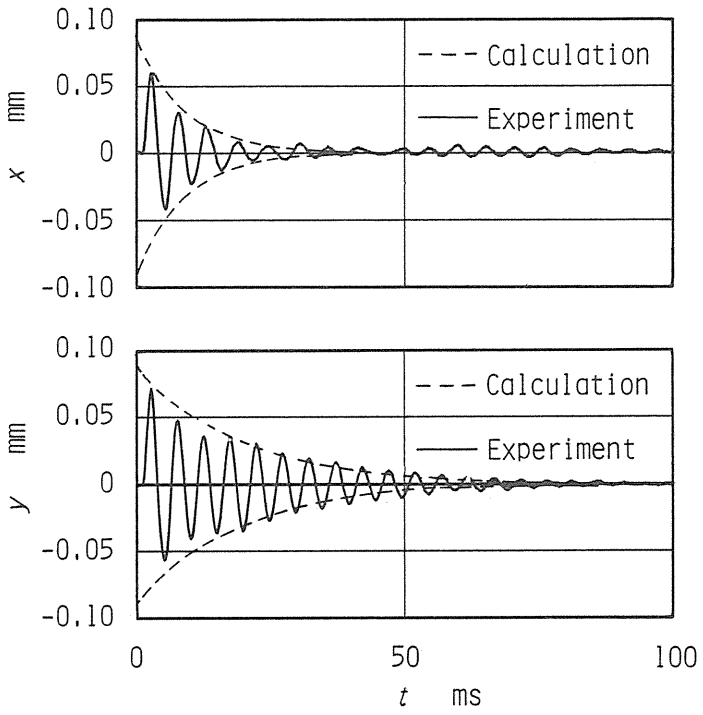

Fig. 2. 3. Natural vibrations of workpiece

2. 4. 2. Characteristics of cutting force

Under stable cutting conditions, cutting forces and deflections of the workpiece were measured from the start of the cutting operation. Then the cutting forces F_x and F_y are related to an instantaneous depth of cut. Fig. 2. 4 shows the typical relations for various feed rates d_0, and for workpieces of 2 or 3 mm in width at a constant cutting speed of 150 m/min. In Fig. 2. 4, cutting forces don't depend on the feed rate but depend on the instantaneous depth of cut. As pointed out by Albrecht,[24] the cutting forces F_x and F_y approach straight lines as the depth of cut increases. Fig. 2. 5 shows a plot of the cutting force versus cutting speed for workpieces of widths 2 and 3 mm at a constant feed rate of 0.125 mm/rev. In this figure, both components of the cutting force decrease by 20 % with a 100 % increase of the cutting speed from 100 to 200 m/min. Indeed, Fig. 2. 5 shows that the cutting forces changed only by 2 % for a change of cutting speed by 10 % being the maximum change of cutting speed in the experiments. Hence, the authors neglected the effects of vertical velocity $\dot{y}$ on the cutting force and then applied the relation between the cutting forces and the depth of cut (Fig. 2. 4) to Eq. (6).

2. 4. 3. Growth of chatter vibration

Fig. 2. 6 shows the typical experimental results of the horizontal deflection of the workpiece. In these figures, the abscissa is the rotating angle θ and the ordinate is the horizontal deflection x. Here, θ is defined as following: at $\theta=0$, the cutting operation starts; when θ is in a range of $2N\pi \leqq \theta < 2(N+1)\pi$, θ is defined as the Nth revolution

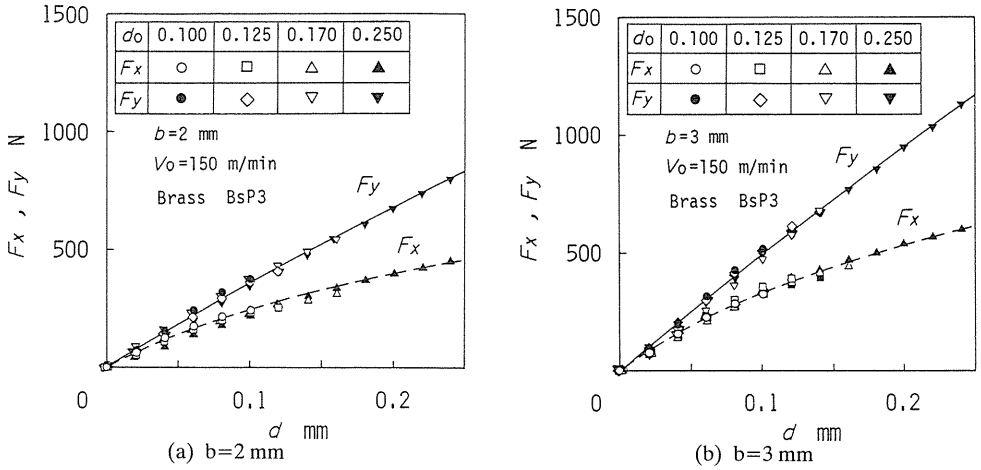

(a) b=2 mm (b) b=3 mm

Fig. 2. 4. Effect of depth of cut on cutting forces

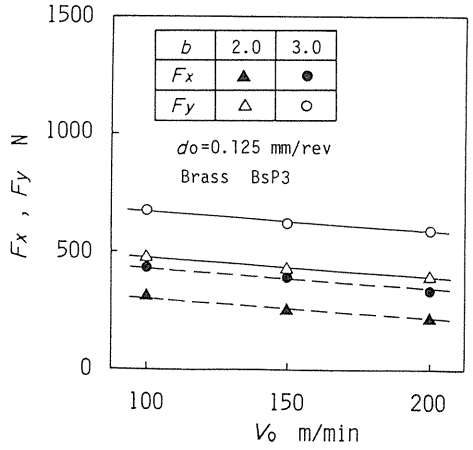

Fig. 2. 5. Effect of cutting speed on cutting forces

and x is shifted downward by Nd_0 in Fig. 2. 6, where N=0, 1, 2, ..., 7. Figs. 2. 6(a) and (b) show examples with chatter, and Fig. 2. 6(c) without chatter. In Fig. 2. 6(b), small disturbances of amplitude of about 2 μm appear at points A_1, A_2 and A_3 in a short time. However, they increase their amplitude with every rotation due to a regenerative effect. When turning our eyes to points B_1, B_2, B_3 in Fig. 2. 6(c), we also find out these small disturbances exist even in a stable cutting condition.

In previous researches on regenerative chatter,[4-10,19,20] many researchers paid attention only to the characteristics of chatter vibration when it had grown up, because of the difficulty of measurement. However, from these experimental facts, the authors conclude that regenerative chatter grows in the following fashion. First, small changes of the cutting force, which may be caused by inclusions in a material or the lack of uniformity of the

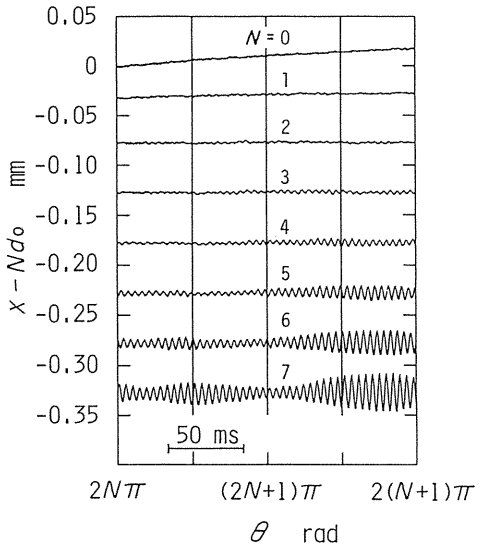

(a) b=2 mm, d_0=0.05 mm/rev

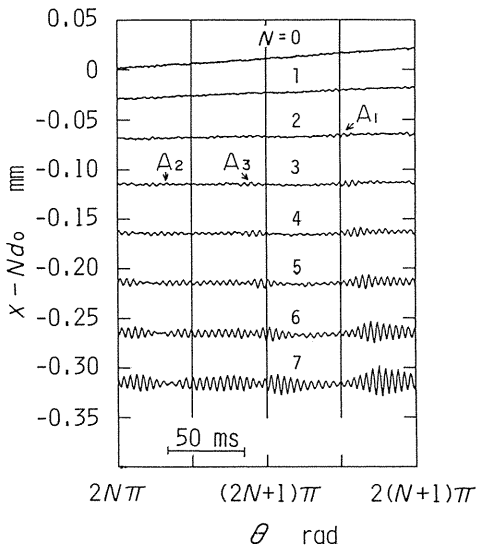

(b) b=3 mm, d_0=0.05 mm/rev

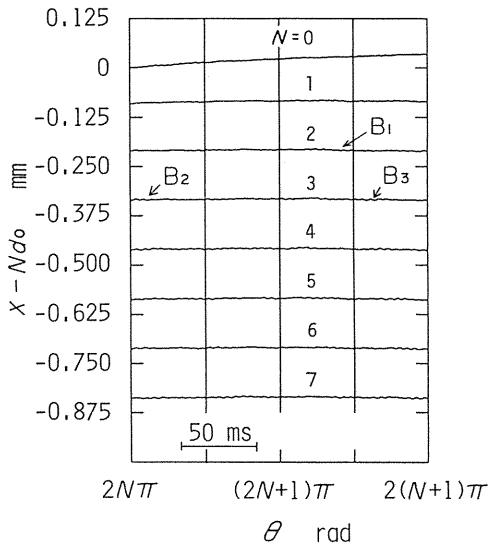

(c) b=2 mm, d_0=0.125 mm/rev

Fig. 2. 6. Growth of horizontal vibration of workpiece
(Experimental results, V_0=150 m/min)

material and exist even in stable cutting conditions, cause small vibrations of the workpiece. These vibrations disappear in a short time but leave short wavinesses on the workpiece surface. Second, in an unstable cutting condition, these small wavinesses

increase their amplitude to spread over the workpiece surface, with every rotation, due to a regenerative effect.

Previous investigators assumed that waviness of a small amplitude existed uniformly on the whole surface of a workpiece at a stability limit and increased its amplitude in unstable cutting conditions. Above experimental results, however, show that previous assumption is not good in the usual cutting condition where rigidity, the damping coefficient and the natural frequency of a workpiece are as high as these experiments.

Next, the authors compared these experimental results with the calculated results for a case where the workpiece suffered a small disturbance. Figs. 2. 7(a) and (b) show the results calculated numerically using the Gear method from Eq. (6) under the following conditions: vibratory parameters are as shown in Table 2. 1; cutting conditions are the same as those for Figs. 2. 6(a) and (b). Further, following initial conditions are chosen: $x(0)=x_0+2\,\mu$m, $y(0)=y_0$, $\dot{x}(0)=\dot{y}(0)=0$ m/s, where x_0, y_0 are steady state deflections of the workpiece for $d=d_0$.

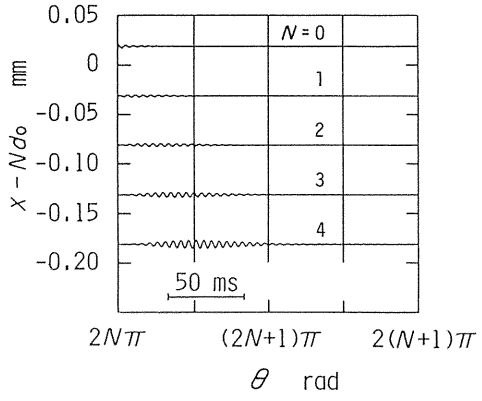

(a) $b=2$ mm

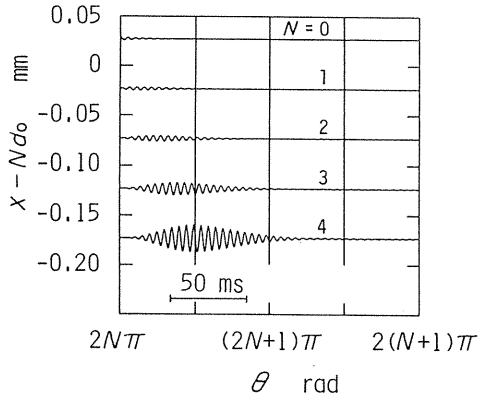

(b) $b=3$ mm

Fig. 2. 7. Growth of horizontal vibration of workpiece (Calculated results, $d_0=0.05$ mm/rev and $V_0=150$ m/min, using with the vibratory parameters shown in Table 2. 1 and the following initial conditions: $x(0)=x_0+2\,\mu$m, $y(0)=y_0$, $\dot{x}(0)=\dot{y}(0)=0$ m/min)

Theoretical results in Figs. 2. 7(a), (b), agree well with the experimental results in Figs. 2. 6(a), (b). This agreement confirms that a small disturbance which exists even in a stable cutting condition can cause regenerative chatter. Yet there remain small differences between experimental and calculated results. Maybe these differences are caused by neglecting the effects of both the radius of the cutting edge and the friction at the cutting edge or by using the incorrect value of the vibratory characteristics of the workpiece.

Fig. 2. 8 shows how deflections of the workpiece x and y, the cutting forces F_x and F_y, and the energy of vibratory system E and E_s change during 50 ms. In this figure, an instant (t=0) corresponds to a rotation angle $\theta/2\pi$=6.75 in Fig. 2. 6(b). Here, the total energy E is the input energy due to cutting forces subtracted by dissipation energy. The energy of the vibratory system E_s is a sum of the elastic energy and the kinetic energy of the workpiece. Let E and E_s be equal at t=0. The calculations and comparisons of E and E_s have the following meanings. First, the authors can relate deflections of the workpiece or cutting forces to the change of total energy E. When E has a different value after one revolution, E makes the amplitude of deflection increase or decrease. Second, it is a good criteria of vibratory parameters of the workpiece in order to estimate the accuracy of the experiments. Because E is calculated with the different values from that for calculation of E_s, if these values are not of good accuracy, E may have quite a different value from E_s under a certain condition.

Fig. 2. 8 shows a small difference between E and E_s to confirm the good accuracy of vibratory parameters shown in Table 2. 1. Further, Fig. 2. 9 shows the following relations between deflections and cutting forces: (1) the workpiece moves in the clockwise direction along an oblique line with a positive slope [left upper figure]; (2) the cutting force changes along an oblique line with a positive slope in the counter-clockwise direction [left lower figure]; (3) the right two figures, both upper and lower, show loci in the clockwise direction along an oblique line with a negative slope. This means that cutting forces increase the energy of the vibratory system.

Though these characteristics have been pointed out by many researchers,[7,20] the regenerative effect on the chatter vibration and the relations between the cutting forces and the deflections of the workpiece were not sufficiently determined.

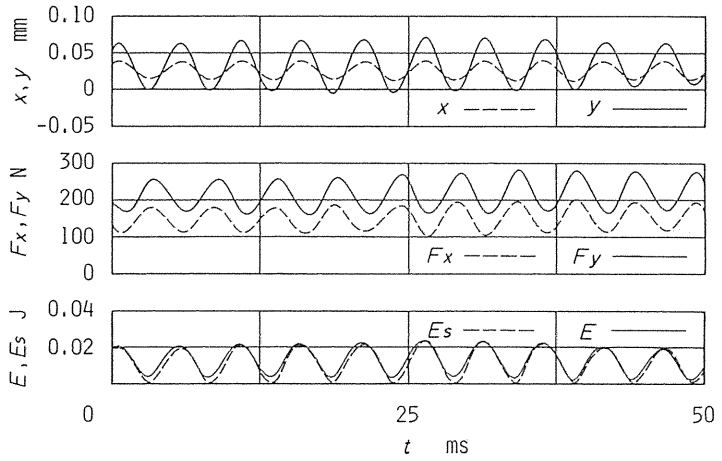

Fig. 2. 8. Changes of workpiece deflections, cutting forces and total energy (Experimental results, b=2 mm, d_0=0.05 mm/rev, V_0=150 m/min)

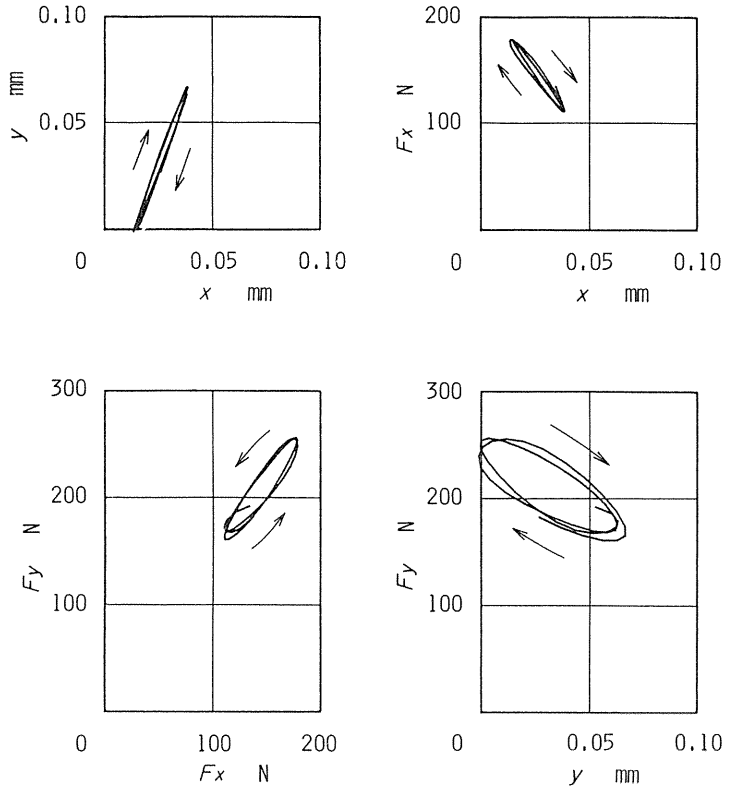

Fig. 2. 9. Relations between workpiece deflections and cutting forces (Experimental results, b=2 mm, d_0=0.05 mm/rev, V_0=150 m/min)

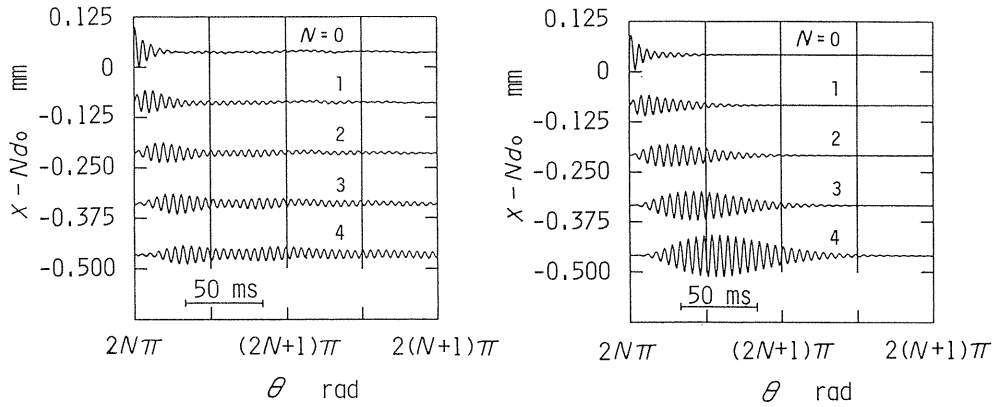

(a) Experimental result

(b) Calculated result

Fig. 2. 10. Growth of horizontal vibration of workpiece (b=2 mm, d_0=0.125 mm/rev, V_0=150 m/min, calculated by the vibratory parameters shown in Table 2. 1 and the following initial conditions: $x(0)=x_0$, $y(0)=y_0$, $\dot{x}(0)$=0.067 m/s, $\dot{y}(0)$=0 m/min)

2. 4. 4. Results with disturbance by a hammer blow

Under stable cutting conditions, the workpiece is disturbed by a hammer blow. How does this disturbance affect the cutting operation during subsequent revolutions? Fig. 2. 10(a) shows typical experimental results under the condition that b=2 mm, d_0=0.125 mm/rev, V_0=150 m/min and the workpiece is disturbed at θ=0. Similarly, Fig. 2. 10(b) shows a calculated result under the same cutting conditions. The initial conditions are the following: $x(0)=x_0$, $y(0)=y_0$, $\dot{x}(0)$=0.067 m/s and $\dot{y}(0)$=0 m/s, where x_0, y_0 have the same definition as in Fig. 2. 7. Fig. 2. 10(b) shows that a chatter mark left by an initial

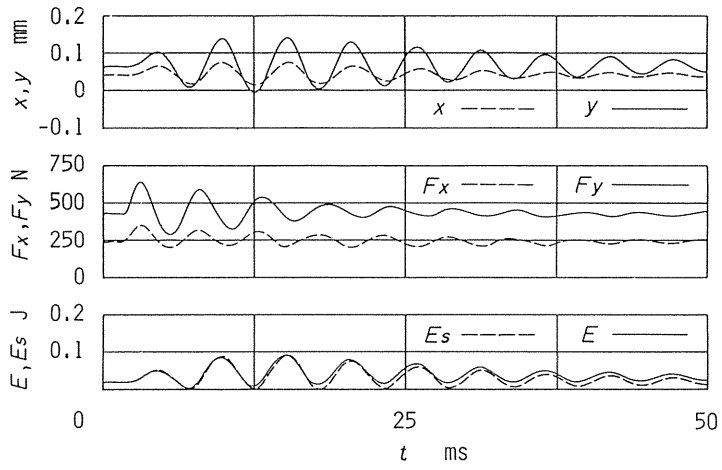

(a) Experimental result

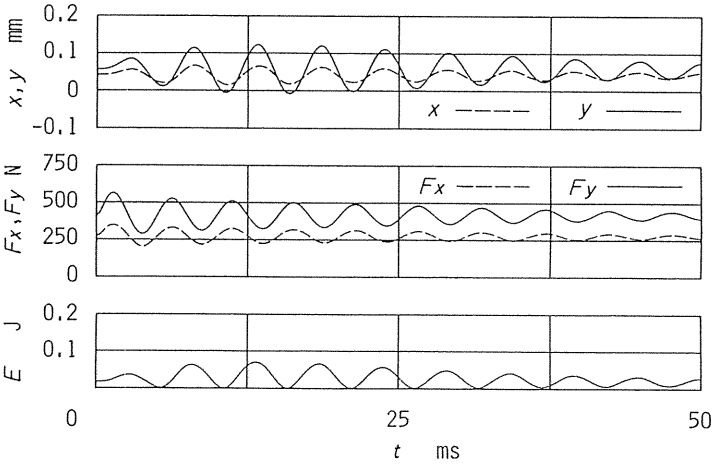

(b) Calcultated result

Fig. 2. 11. Changes of workpiece deflections, cutting forces, and energy (b=2 mm, d_0=0.125 mm/rev, V_0=150 m/min)

disturbance on a workpiece surface spread over the workpiece surface, with every rotation, due to a regenerative effect. This manner is similar to that in Fig. 2. 10(a).

Fig. 2. 11(a) shows, in more detail, the characteristics of regenerative chatter represented in Fig. 2. 10(a). It illustrates how deflections of the workpiece x and y, the cutting forces F_x and F_y and energy of the system E and E_s change during 50 ms. In the figure, E agrees well with E_s. It is then verified that the experiment is also in good accuracy under the condition where a workpiece suffers a disturbance by a hammer blow. In Figs. 2. 11(a) and (b), an instant (t=0) corresponds to the rotation angle $\theta/2\pi$=1, as in Figs. 2. 10(a) an (b). Figs. 2. 12(a) and (b) show the relation between the deflections x and y, and the cutting forces F_x and F_y represented in Figs. 2. 11(a) and (b). Previous investigator[7,20] failed to determine whether the workpiece moved in a clockwise or counterclockwise direction. However, the authors can explain through Eq. (6), why this contradiction takes place. First, let α=0° in Eq. (6) and consider the situation where no elastic coupling exists between two axes x and y. Eq. (6) tells us that the horizontal cutting force acts as a kind of spring force, increasing the horizontal natural frequency. However, the vertical cutting force acts as a external force, thus causing no change in the

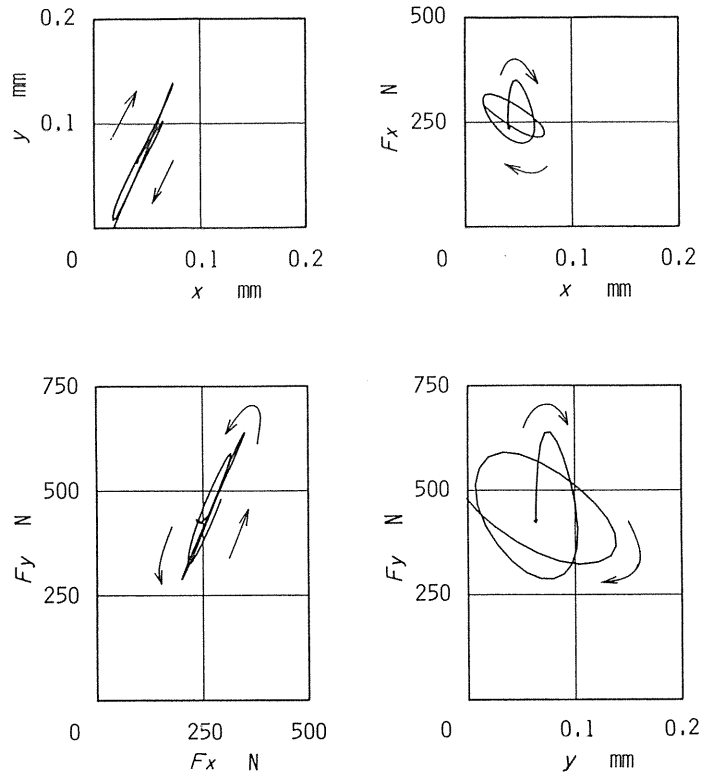

(a) Experimental result

Fig. 2. 12. Relations between workpiece deflections and cutting forces (b=2 mm, d_0=0.125 mm/rev, V_0=150 m/min)

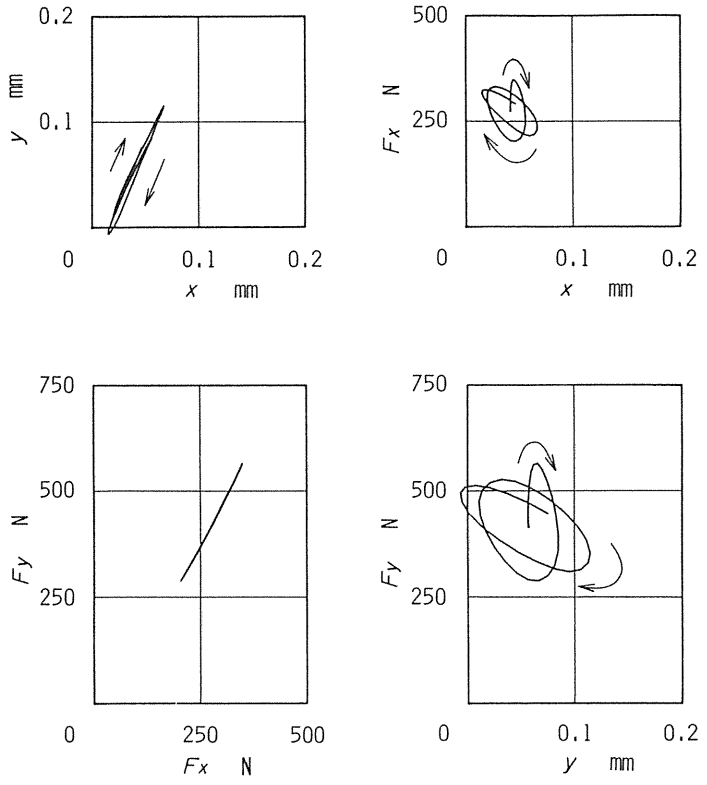

(b) Calculated result

Fig. 2. 12. Relations between workpiece deflections and cutting forces (b=2 mm, d_0=0.125 mm/rev, V_0=150 m/min)

natural frequency in the vertical direction. Now we consider the case that under a cutting operation, Δ_k has a negative value sufficient to keep the vertical natural frequency higher than the horizontal one. Eq. (6) tells us that, in this case, Δ_k makes a phase lag of the vertical displacement behind the cutting force smaller than that of the horizontal displacement and then makes the workpiece move in the clockwise direction. Further, estimating the effect of Δ_k and α on chatter vibration by evaluating Eq. (6) numerically for various values, the authors verified the effect of Δ_k and found a secondary effect of α on chatter vibration.

Finally, the right upper and the right lower figures in Figs. 2. 12(a) and (b) show that cutting forces increase their value initially and then make the workpiece move in clockwise direction along a line with negative slope. In this case, deflections lag 130° in phase behind the cutting forces (see Figs. 2. 11(a), (b)). On the whole, experimental results agree with results calculated numerically from Eq. (6) with the cutting force characteristics shown in Fig. 2. 4. This good agreement gives a key to the investigation of the transient behavior of regenerative chatter vibration. However, the dynamics of the cutting forces shown in Fig. 2. 12(b) are somewhat different from that in Fig. 2. 11(b) because only the static characteristics of cutting force are in consideration.

Chapter 3. Effects of Cutting Edge with Positive Rake Angle on the Chatter Vibration of a Workpiece[31)]

3. 1 Introduction

In the workshop, we have often encountered the case that the chatter builds up and stops a cutting operation soon after the cutting operation has begun. Previous investigations[12,13)] for prediction of chatter were based on the assumption that the properties of cutting forces did not depend on the cutting conditions, i.e. cutting speed or feed rate. These depending properties were specific cutting force,[12,13)] time lag of the cutting force[13)] and the penetration effect.[12)] Another previous works revealed the condition under which the chatter vibration occurred and indicated the characters of chatter itself when the cutting forces had non-linear characters, especially the non-linearity of the specific cutting force[25,26)] or a multi-regeneration effect.[19)]

On the other hand, there were another approaches of revealing the physical causes of the chatter vibration through a experiment. Hahn[2)] reported that the friction between a tool and a chip in the initial stage of a cutting operation was one of the causes of chatter and that no chip was generated in the region marked rubbing. Yuta[27)] indicated that in the initial stage of the cutting operation there were three regions: the first region was the rubbing, the second one the rubbing-cutting transition and the third one the cutting region. And he also indicated that in the rubbing or the rubbing-cutting transition region the cutting forces showed the different characters from that in the cutting region. Yamamoto and Nakamura[28-30)] showed a significant effect of the cutting edge on the condition under which the cutting operation began.

Above experimental results showed that the cutting dynamics depended on the depth of cut or the configuration of a tool, and that static and dynamic cutting forces depended on the depth of cut. Further, these experiments showed that previous theoretical works for the prediction of chatter didn't provide a sufficient result for the problem in milling or in finishing with a wear tool because theoretical works only took into account a static cutting force.

In this chapter, through experiments the authors first indicated how the depth of cut and the configuration of the tool affected on static or dynamic cutting force. Next, the authors revealed the physical causes of chatter which included the chatter affected by the non-linearity of the cutting forces or the chatter affected by the friction between a surface of a workpiece and a tool.[31)]

3. 2 Experimental results

Fig. 3. 1 shows how deflections of the workpiece x and y, the cutting forces F_x and F_y and the depth of cut d change during 800 ms. In the figure, three marks ∇ are plotted. The first mark shows the start of the cutting operation, the second showing a first half rotation of a workpiece and the third showing one rotation.

Previous researches reported that in the initial stage of the cutting operation the chatter vibrations were caused by the friction between a cutting edge and a workpiece. The authors verified that the chatter vibration appearing in Fig. 3. 1 occurred after the cutting operation had begun and further the chip had been formed. For detecting the chip formation, the authors used the sensor Ⓢ installed on the tool edge and adjusted to make the signal when the chip touched the sensor. Fig. 3. 2 illustrates this sensor. The mark $\Uparrow$, in Fig. 3. 1, represents the instant when the chip touches the sensor. Our experiments confirm that after the chip has been formed the chatter vibration occurs. Moreover, this

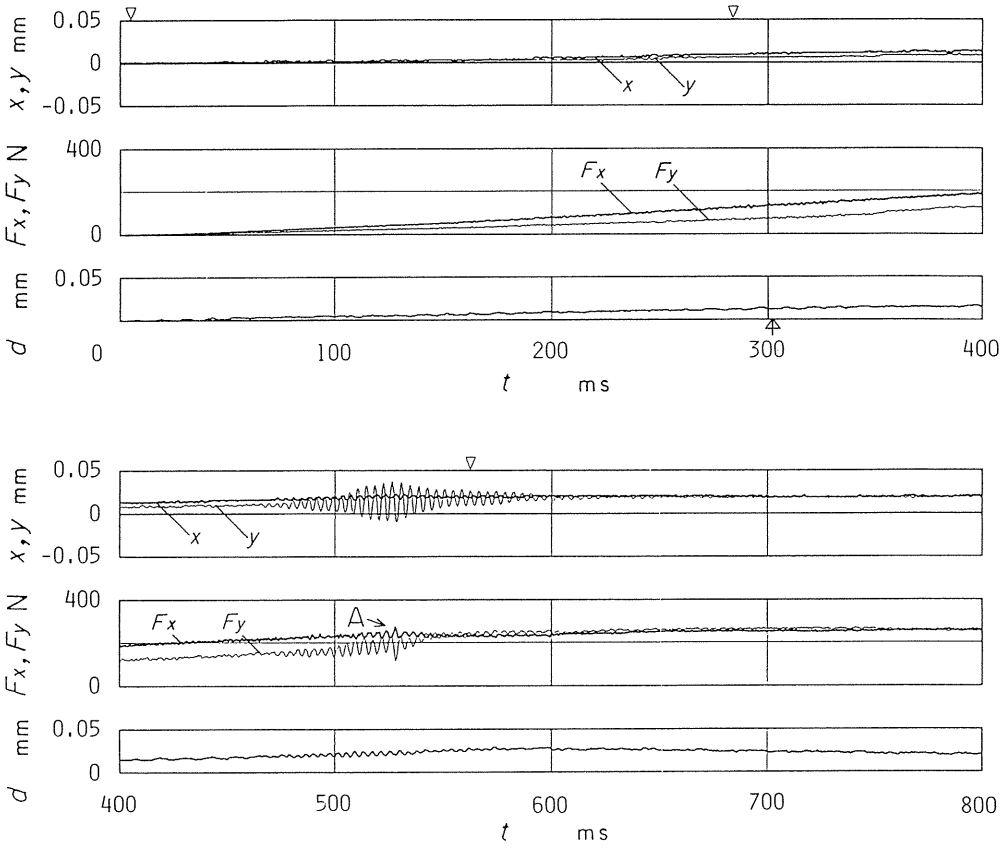

Fig. 3. 1. Example of chatter vibration (d_0=0.05 mm/rev, V_0=50 m/min)

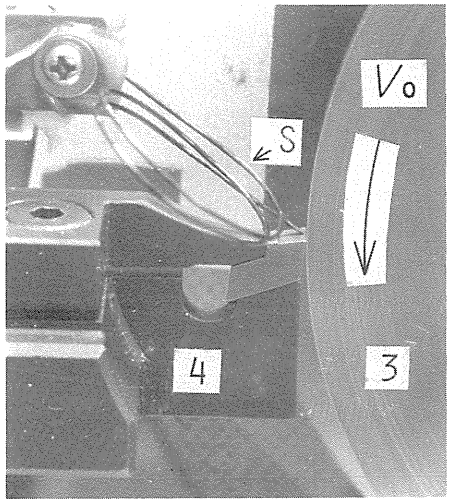

Fig. 3. 2. Photograph of workpiece ③, tool ④ and sensor Ⓢ

fact means that the impact which a tool ④ exerts a workpiece ③, or the friction between a tool and a workpiece has no attribution to chatter.

In Fig. 3. 1, at t=470 ms (the depth of cut d=19 μm) the vertical displacement y and the vertical cutting force F_y begin to fluctuate and at t=540 ms (d=25 μm) the vertical cutting force stops to fluctuate. These characteristics were also reported by Hahn.[2)]

3. 2. 1. Static characteristics of cutting forces

Now, the authors show the static characteristics of the cutting forces common with and without chatter. Fig. 3. 3(a) shows the typical relations between the cutting forces F_x, F_y and the depth of cut d for various feed rates (d_0=0.05~0.25 mm/rev) and a constant cutting speed (V_0=75 m/min). Also, Fig. 3. 3(b) shows the typical ones for various cutting

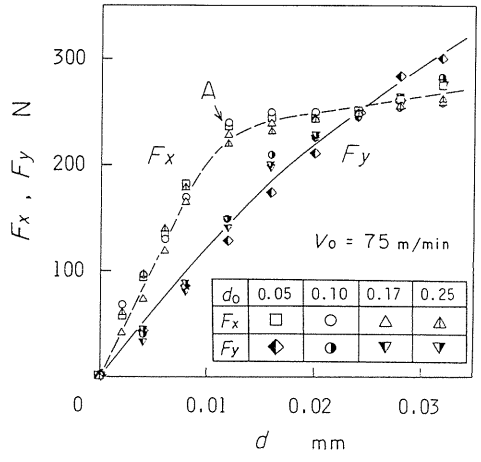

(a)

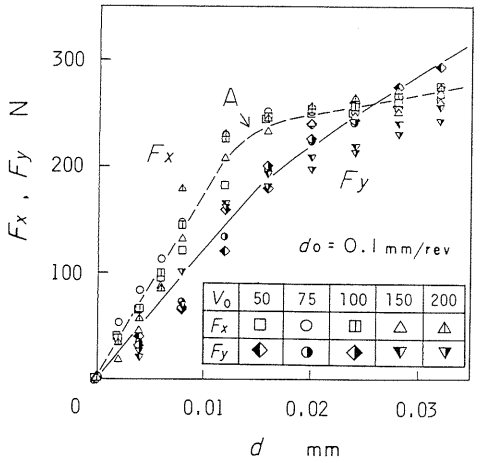

(b)

Fig. 3. 3 Effect of depth of cut on cutting forces

speeds (V_0=50~200 m/min) and a constant feed rate (d_0=0.1 mm/rev). The authors already eliminated the part where the chatter vibration occurred from both figures. Figs. 3. 3(a) and (b) show two characteristics. The first characteristic is that the both cutting forces F_x and F_y do not depend on the feed rates or the cutting speeds but depend on the depth of cut. The second is that the horizontal cutting force F_x increases nonlinearly as the depth of cut increases. This nonlinearity was also reported in other investigations[26,29] in which the workpiece was steel.

To compare these results to the experimental results obtained in Chapter 2 (see Figs. 2. 4(a), (b) and Fig. 2. 5), the authors illustrate Fig. 3. 4 and Fig. 3. 5. Fig. 3. 4 shows that the cutting forces F_x and F_y don't depend on the feed rate but depend on the depth of cut also in the range of the depth of cut $0<d<0.25$ mm. Fig. 3. 5 shows the relation between the cutting forces F_x, F_y and the cutting speeds at a depth of cut $d=d_0$ and a feed rate d_0=0.1 mm/rev. In Fig. 3. 5, we also recognize that the vertical cutting force F_y decreases as the cutting speed increases. The authors rearrange the data presented in Fig.

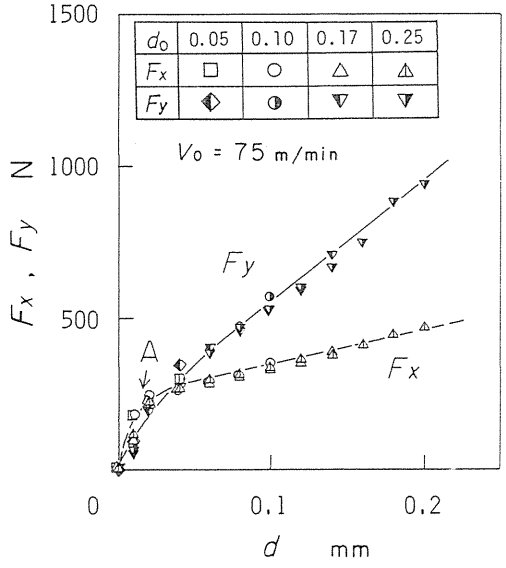

Fig. 3. 4. Effect of depth of cut on cutting forces

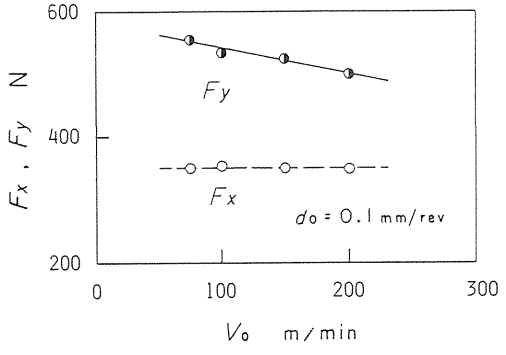

Fig. 3. 5. Effect of cutting speed on cutting forces

3. 3(b) and illustrate a plot of the vertical force F_y versus the horizontal cutting force F_x in Fig. 3. 6. In this figure, the cutting force F_y increases along two straight lines P, Q as the cutting force F_x increases. Yuta[27] explains that as the cutting forces F_x and F_y increase along a line P, first the cutting edge rubes a workpiece and then the rubbing-cutting transition takes place. At the same time in the transition region the chip begins to flow out. This point is marked with an arrow ↟ in Fig. 3. 6. Yamamoto and Nakamura[28] or Yuta[27] named this point as the start of the cutting operation. Fig. 3. 7 shows the experimental value of the depth of cut at which the cutting operation begins.

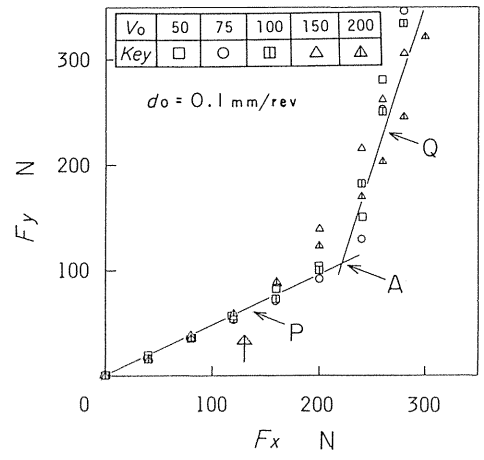

Fig. 3. 6. Relation between vertical cutting force F_y and horizontal cutting force F_x

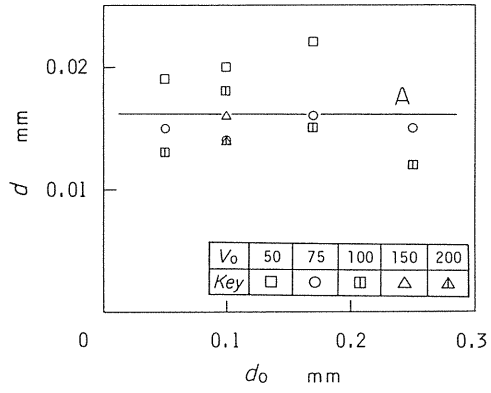

Fig. 3. 7. Depth of cut at a start of cutting operation

3. 2. 2. Conditions under which chatter vibrations occur

In Chapter 2 the authors already reported[21,22] that in the initial stage of the cutting operation the static characteristics of the cutting force do not depend on the cutting condition but depend on the depth of cut. In contrast this fact, the chatter vibration occurs depending on the cutting conditions. Now let's consider the physical cause of this character. Fig. 3. 8 shows the depth of cut d_s, d_e, where the depth of cut d_s is the depth at which the chatter vibration begins and the depth of cut d_e is one at which the chatter vibration ceases. In this figure, the depth of cut d_s has the almost same average value as one which Fig. 3. 7 presents for the start of the cutting operations. This fact tells us the close connection between the physical causes of chatter and the cutting operation in this stage. So, the authors observed by use of a high speed camera how the chip flowed out of a workpiece. Further the authors evaluated the following parameters: (a) the radius of

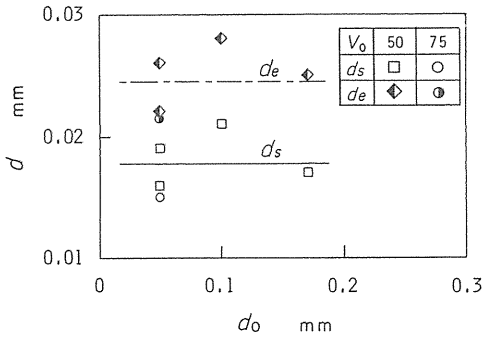

Fig. 3. 8. Depth of cut d_s, d_e: chatter occurs at $d=d_s$ and ceases at $d=d_e$.

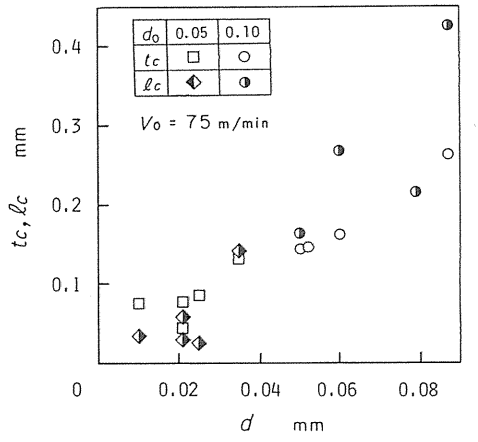

Fig. 3. 9. Effect of depth of cut on chip thickness and contact length

the cutting edge of a tool r (in our experiments $r=70\,\mu$m); (b) the ratio of the chip thickness to the depth of cut t_c/d; (c) the ratio of the contact length of the chip with a tool on the rake face to the depth of cut l_c/d (see Fig. 3. 9).

On the basis of these experiments, the authors illustrate the manner how the chip flows out of a workpiece as the depth of cut increases by Figs. 3. 10(a), (b), (c) and (d). Fig. 3. 10(a) is for an instant when the chip begins to flow out, Fig. 3. 10(b) for an instant when the chatter vibration occurs, Fig. 3. 10(c) for an instant when the chatter vibration ceases, and Fig. 3. 10(d) for an instant when the depth of cut has been thicker than that in Fig. 3. 10(c). The cutting operation changes in the following way. First, the chip is bended at the round cutting edge and flows out of a workpiece at a angle $\psi=45°$ to the surface of a workpiece (see Fig. 3. 10(a)). As the depth of cut increases, the chip flows out at a larger angle. Finally, the chip flows out along a rake face of a tool (see Fig. 3. 10(c)). The curing of the chip doesn't appear in Figs. 3. 10(a) and (b). The observations of a high speed camera taught us; (1) when the chatter vibration occurred the chip flowed out with a fluctuating angle; (2) the instant when the chip began to flow out along a rake face agreed with the instant when the cutting operation began (see Fig. 3. 7); (3) after this instant, the chip flowed out rapidly. Also these observations indicated

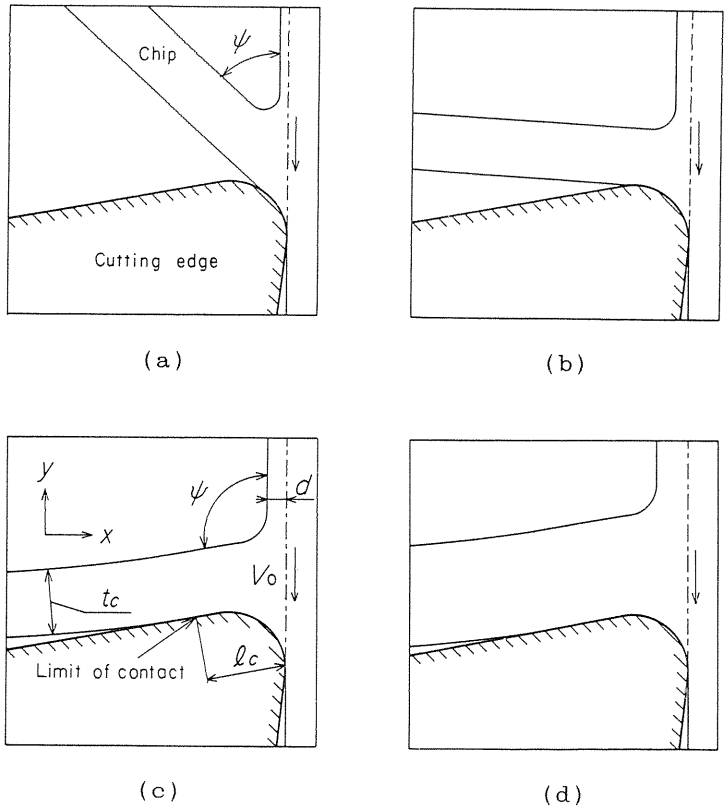

Fig. 3. 10. Flow pattern of generated chip

the same results reported by Yuta[27] or Yamamoto and Nakamura,[28] i.e., at the depth of cut marked with A in Fig. 3. 7, the cutting operation began.

Fig. 3. 11 shows the stress distribution[28] on the round edge of a tool at the instant represented by Fig. 3. 10(b). According to Fig. 3. 10(b), Fig. 3. 11 and the results on a tool which has a large negative angle,[32] the chatter vibration occurs in the following way. Here, we consider only the vertical component of chatter because in our experiments the horizontal component of chatter is negligible and the horizontal component of the cutting force F_x increases slightly over the depth of cut where the chatter vibration occurs.

(1) First, let imagine the case that a workpiece is disturbed and moves downward ($\dot{y}<0$, $|\dot{y}| \ll V_0$).

(2) This movement increases the cutting speed from V_0 to $V_0-\dot{y}$ and increases the shearing force acted between the rake face of the cutting edge and the chip (see Fig. 3. 11). This increase of shearing force makes the chip flow out at a lager angle.

(3) The chip to flow out at a lager angle has the same effect as the increase of the rake angle[32] and then reduces the plastic deformation zone and the vertical cutting force.

(4) The reduction of the vertical cutting force makes a workpiece move downward more.

(5) When a workpiece is disturbed and moves upward ($\dot{y}>0$, $|\dot{y}| \ll V_0$), the shearing force and a angle at which the chip flows out decreases. Finally the increase of the vertical cutting force takes place and then makes a workpiece move upward more.

Upon these consideration, we can conjecture the following phenomena.

(i) When a workpiece moves upward ($\dot{y}>0$), the vertical cutting force increases from F_y to $F_y+\Delta F_y(\Delta F_y>0)$. When a workpiece moves downward ($\dot{y}<0$), the vertical cutting force decreases from F_y to $F_y+\Delta F_y(\Delta F_y<0)$.

(ii) The chatter vibration doesn't occur under the condition illustrated in Fig. 3. 10(a) because under this condition the shearing force and the amount of its fluctuation are relatively small and then a angle at which the chip flows out doesn't fluctuate.

(iii) The chatter vibration becomes to cease under the condition that the chip flows out along the rake face of the tool because under this condition the rake face prevents the chip from flowing out with fluctuation.

(iv) Above conjectures (ii) and (iii) imply that the chatter vibration can occur in a certain limited range of the depth of cut.

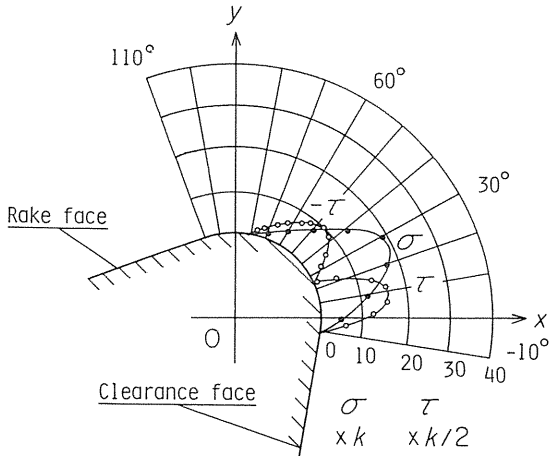

Fig. 3. 11. Distribution of stress on cutting edge
(k is fringe order, after Yamamoto and Nakamura[30])

To verify above conjectures (i) to (iv), the authors attempted the experiments of hitting a workpiece with a hammer in the vertical direction immediately after the cutting operation began. The cutting condition was selected at the critical one that chatter occurred (d_0=0.1 mm/rev, V_0=75 m/min). Fig. 3. 12(a) shows the experimental result in the case that a workpiece is hit at the instant illustrated in Fig. 3. 10(a). Further, Fig. 3. 12(b) is for Fig. 3. 10(b) and Fig. 3. 12(c) is for Fig. 3. 10(c).

In Figs. 3. 12(a) and (c), a fluctuation of the vertical cutting force doesn't appear and the vertical vibrations caused by a hammer blow disappear after a short time. This reslut and the result presented by Fig. 3. 8 verify the above conjectures (ii) to (iv). In contrast this, Fig. 3. 12(b) shows that the vertical deflection y keeps to fluctuate until the depth of cut becomes the depth at which the chip flows out along the rake face of the tool. Fig. 3. 13 shows the relation between F_x and x, and the relation between F_y and y during the time from t=290.5 ms to t=294.5 ms in Fig. 3. 12(b). During this time, the horizontal vibration doesn't appear. Fig. 3. 13 verifies the above conjecture (i), i.e., F_y has the minimum when $\dot{y}$ has the minimum and F_y has the maximum when $\dot{y}$ has the maximum.

Further the conjecture (iv) implies that the amplitude of the chatter vibration depends on the time that the cutting edge passes through an unstable range of the depth

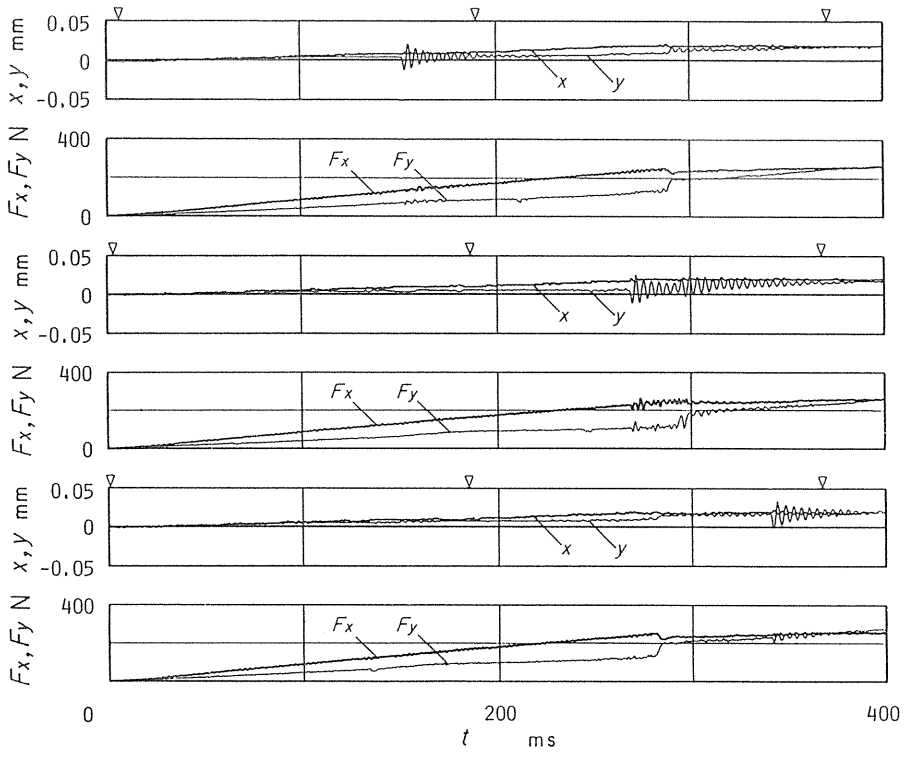

Fig. 3. 12. Example of vibration caused by downward disturbance (d_0=0.1 mm/rev, V_0=75 m/min)

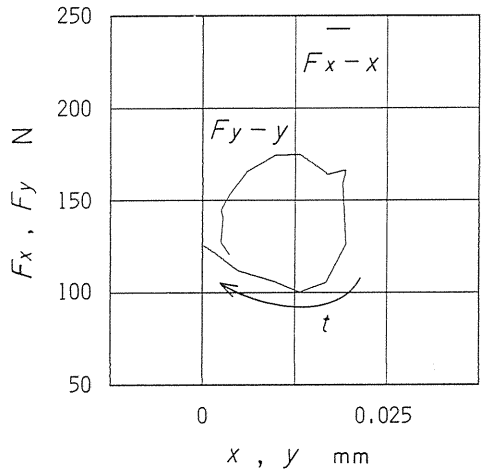

Fig. 3. 13. Relation between cutting forces and deflections of workpiece

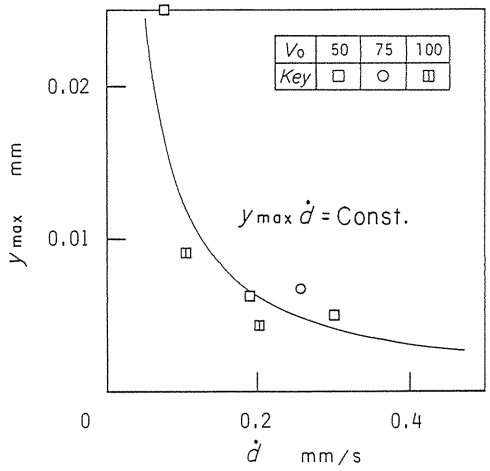

Fig. 3. 14. Relation between chatter amplitude and instantaneous feed rate

of cut. Fig. 3. 14 shows the maximum amplitude of chatter y_{max} versus the instantaneous feed rate $\dot{d}$ obtained in an unstable range of the depth of cut. In Fig. 3. 14, the solid-line curve presents a rectangular hyperbola of $y_{max}\dot{d}$=constant and agrees well with the experimental results. This fact verifies the above implication.

Chapter 4. Effects of the Cutting Edge with Negative Rake Angle on the Chatter Vibration of a Workpiece[33)]

4. 1. *Introduction*

In the Chapter 3, the authors researched experimentally the effects of both the configuration of a tool and the depth of cut on the static or dynamic cutting force with a tool whose rake angle was positive. And the authors indicated the stability chart of chatter and its physical causes. In this chapter, with a tool whose rake angle is negative the authors make similar experiments to the Chapter 3 and indicate two types of physical cause of chatter which occurs in the initial stage of the cutting operation. Further, comparing the results obtained in this chapter with the results obtained in the Chapter 3 the authors show the difference with respect to the stability chart and the physical cause of chatter between two types of tool.[33)]

4. 2. *Experimental results and its consideration*

Fig. 4. 1 shows a typical example with chatter. In the figure, two marks ▽ are plotted. The first mark shows the start of the cutting operation and the second shows first half a rotation of a workpiece. Another mark ↑ represents the instant when the chip was generated and touched the sensor.

The authors compared this figure with Fig. 3. 1 presented in the Chapter 3 and found out the following characteristics.

(1) The horizontal cutting force F_x increases monotonously as time goes on. Its increase rate changes at two points marked with A and B.

(2) The chatter vibrations also appear at these two points. The amplitude of the vertical vibration y is larger than that of the horizontal vibration x.

(3) The chatter vibrations appear only in a limited range of the depth of cut.

In this section, the authors study the physical causes and the mechanism of chatter, and then consider the condition under which chatter occurs.

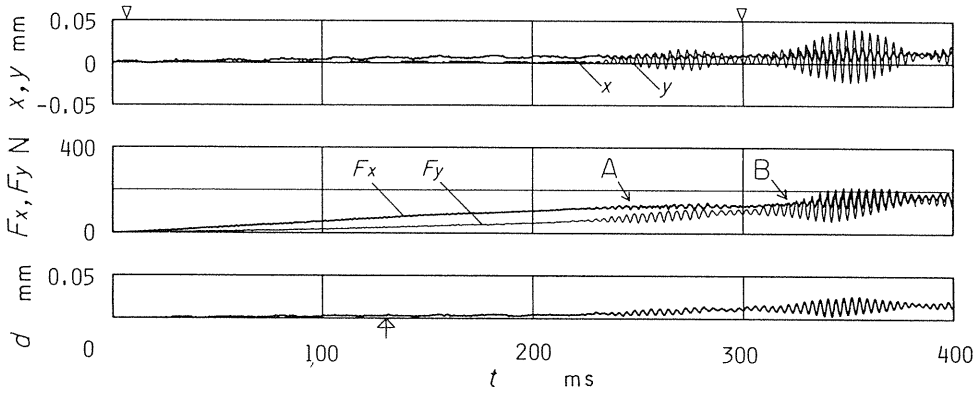

Fig. 4. 1. Example of chatter vibration (d_0=0.05 mm/rev, V_0=50 m/min)

4. 2. 1. Static characteristics of cutting force

First, the authors reveal the characteristics of the cutting forces without chatter. Fig. 4. 2(a) shows the relations between cutting forces and the depth of cut for various feed rates and a constant cutting speed (V_0=75 m/min). Also, Fig. 4. 2(b) shows the similar relations for various cutting speeds and a constant feed rate (d_0=0.1 mm/rev). We rearrange the data presented in Fig. 4. 2(b) and show the relation between F_y and F_x in Fig. 4. 3. Here, the part with chatter is already eliminated from Figs. 4. 2(a), (b) and Fig. 4. 3. The comparisons between these data and the data presented in the previous chapter indicate the characters which these two groups of data have in common and the different characters from each other groups. See Figs. 3. 3(a) (b), Fig. 3. 6, Figs. 4. 2(a) (b) and Fig. 4. 3.

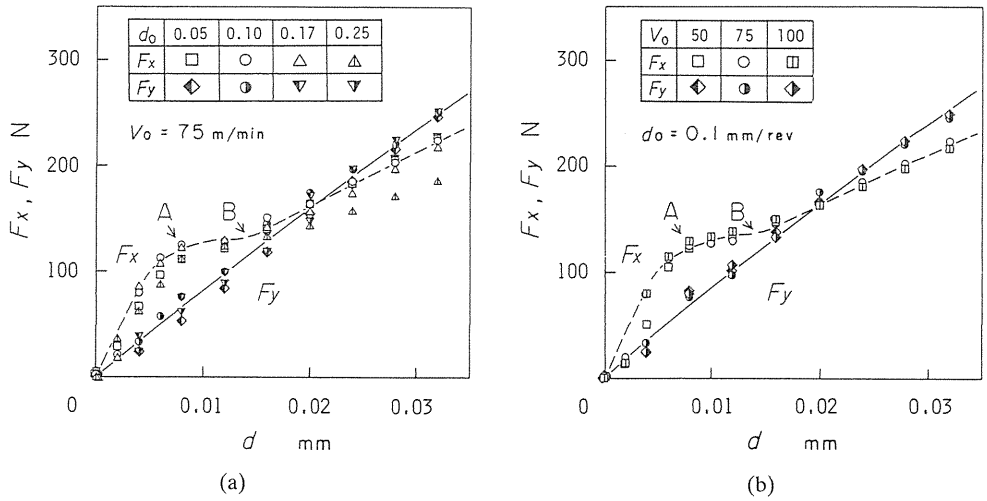

Fig. 4. 2. Effect of depth of cut on cutting forces

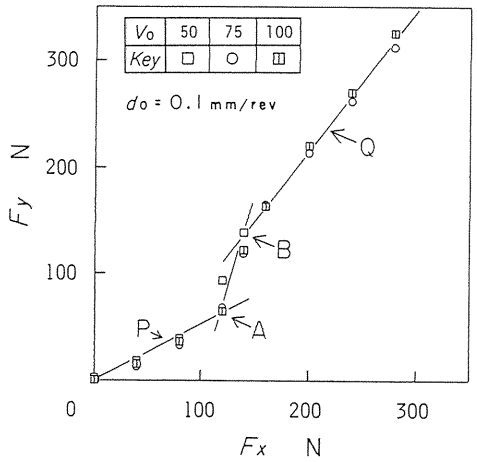

Fig. 4. 3. Relation between vertical cutting force and horizontal cutting force

Common characters:

(1) The cutting forces F_x and F_y don't depend on both the feed rate and the cutting speed but depend on the depth of cut.
(2) Over a range of the depth of cut from $d=0$ to the point denoted by A and above a range of the point denoted by B the increase rate of F_x as a function of d is kept at constant. Further, the increase rate of F_y as a function of F_x equals constant in these two range. With respect to the data presented in the previous chapter (see Figs. 3. 3(a) (b)), the authors identify the point B with the point A.

Different characters:

(1) Both the increase rate of F_x as a function of d and the increase rate of F_y as a function of F_x change at two points marked with A and B.
(2) Above mentioned two increase rates have different values from ones obtained in the previous chapter.

Table 4. 1. Characteristics of cutting forces

Tool		Chapter 4	Chapter 3
Radius of tool edge	r (μm)	36	70
Value at point A	d (μm)	8	18
	F_X (N)	120	200
	F_Y (N)	60	110
Value at point B	d (μm)	14	-
	F_X (N)	130	-
	F_Y (N)	120	-
$\Delta F_Y/\Delta F_X$ along	P	0.53	0.55
	Q	1.3	2.1

Table 4. 1 indicates the cutting forces F_x, F_y and so on at these two points A and B. The values obtained in the Chapter 3 are also seen in this table.

Now, comparing Figs. 4. 2(a), (b), Fig. 4. 3 and Table 4. 1 with the previous works,[24,28,29] the authors will educe the physical meaning of these two points. Among the previous works, Yamamoto and Nakamura[28,29] expressed the following characters of the point at which the cutting operation started.
(1) After the cutting edge touches a workpiece, the increase rate of the cutting force as a function of the cutting length undergoes the first change at this point.
(2) Each of the cutting forces F_x, F_y and the depth of cut d obtained at this point increases in proportion to the radius of the cutting edge.
(3) The cutting forces increase in proportion to the depth of cut over a range from $d=0$ to this point.

(4) The effect of the rake angle on the cutting forces appears above the depth of cut at this point.

The authors have already described that the above characters (1), (2) and (3) also appeared in our experiments. Then, it is confirmed that the point denoted by A is the point at which the cutting operation starts and that the radius of the cutting edge has no effect on the cutting operation over a range between $d=0$ and the depth of cut at the point A. Further, Albrecht[24] expressed that above the depth of cut at the point denoted by B the increase rate of the cutting force as a function of the depth of cut doesn't depend on the radius of the cutting edge but depends on the rake angle. This expression implies that above the depth of cut at point B the rake angle has effects on the cutting operation.

4. 2. 2. Physical causes of chatter

The authors revealed the physical causes of chatter by use of a high-speed camera.

First, the authors observed how the chip flowed out of a workpiece by use of a high-speed camera and found out relations of these observations with the cutting forces or the deflections of a workpiece. Then the authors divided the whole cutting process into following four parts.

(1) From the instant when the cutting edge touched a workpiece to the instant when the chip was generated. During this time the cutting edge rubbed a workpiece.

(2) From the instant when the chip was generated to the instant denoted by the point B. The straight chip without curl was generated. The chip flowed out of a workpiece at an angle of ψ, which varied from 45° to 85° as time went on. At a angle of 85° the chip flowed out along the rake face. When chatter occurred at the point A, the angle at which the chip flowed out fluctuated.

(3) From the instant denoted by the point B to the instant when the chatter ceased. Above the depth of cut at the point B the chip flowed out rapidly along the rake face of a tool with curl. When chatter occurred, the chip flowed out along a rake face with a motion like a stick-slip vibration.

(4) After the chatter ceased. The chip flowed out smoothly with curl of which radius was constant.

It is confirmed that among these four parts the first part conforms the rubbing region and the second part conforms the part from the rubbing-cutting transition to the initial cutting region.[27] This result agrees with the result which the authors indicated in the Chapter 3. So, it is also confirmed that chatter which occurs at the point A is the same chatter as the authors showed in the Chapter 3.

However, in the following three aspects the cutting condition from the third to fourth part is different from that which the authors showed in the Chapter 3. First, though in the Chapter 3 the chip flowed out rapidly above the depth of cut at the point A, in this chapter the chip flows out rapidly above the depth of cut at the point B. Second, above the depth of cut at the point B the horizontal cutting force F_x increases as the depth of cut increases. Third, chatter occurs in the third part. Among these differences, the first and the second come from the difference of a rake angle. The larger a rake angle becomes, the more difficult the chip flows out along a rake face, which causes the first difference. Further, the direction and magnitude of the cutting force acted on a rake face and also the increase rate of the cutting force as a function of the depth of cut depend on a rake angle. Which causes the second difference.

On the other hand, the third difference depends on the cutting dynamics. So, the authors searched the cutting dynamics and revealed the physical causes of this chatter.

Fig. 4. 4(a) shows the relation of F_x to x during a time from t=335 ms to t=339 ms in Fig. 4. 1 and Fig. 4. 4(b) shows the relation of F_y to y during the same time. Fig. 4. 1, Figs. 4. 4(a) and (b) illustrate that, in spite of the damping of the x direction, chatter increases its amplitude due to the supply of energy in the y direction. When the system has an elastic coupling, the energy can be supplied from a vertical motion into a horizontal motion. However, an elastic coupling doesn't excite a self-sustained oscillation. So, the authors consider that the system is coupled through the cutting operation and this type of coupling excites an oscillation. Following experiments were carried out to confirm this consideration. In our experiments, after the cutting operation had begun, the authors hit a workpiece downward with a hammer at the depth of cut at which chatter occurred. Here the authors cut a workpiece at the critical cutting condition (d_0=0.075 mm/rev, V_0=75 m/min). Fig. 4. 5 illustrates how x, y, F_x, F_y and d change as time goes on. At the time denoted by the mark △, a workpiece is disturbed by a hammer blow.

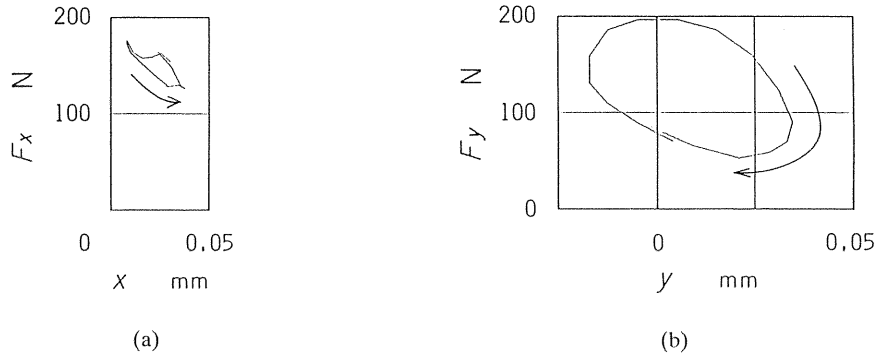

Fig. 4. 4. Relation between cutting force and deflection (d_0=0.05 mm/rev, V_0=50 m/min)

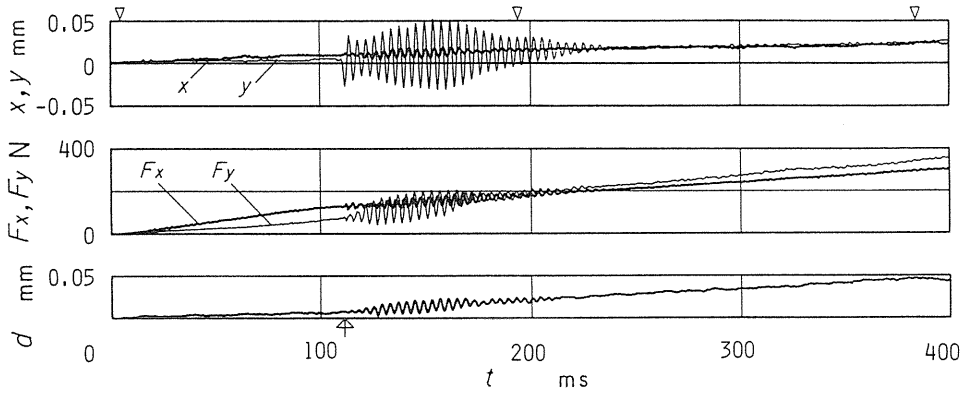

Fig. 4. 5. Example of vibration caused by downward disturbance

Also, Fig. 4. 6 shows the relation of F_x to x or y immediately after a disturbance during a time from t=115 ms to t=119 ms. In this figure, it is confirmed that the cutting

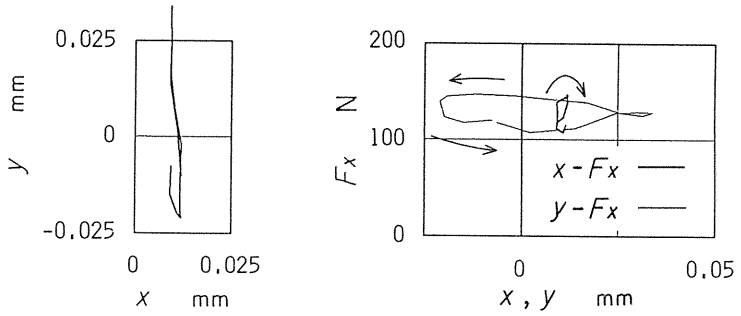

Fig. 4. 6. Relation between cutting force and deflection

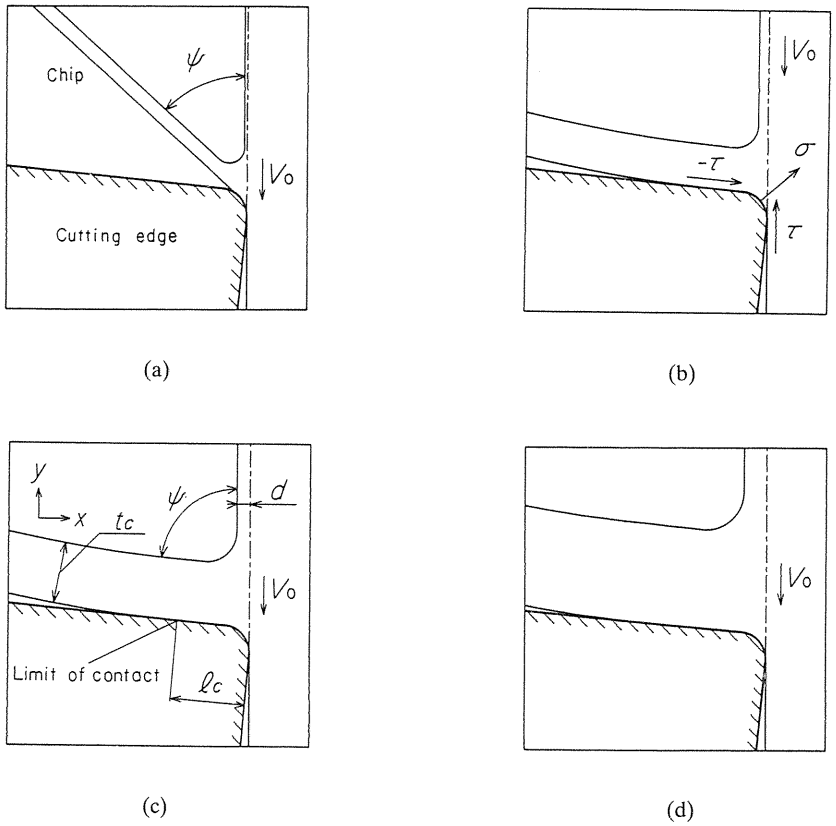

Fig. 4. 7. Flow pattern of generated chip

operation couples the vertical motion to the horizontal motion. In other words, the horizotal cutting force F_x in a downward motion ($\dot{y}<0$) is larger than that in an upward motion.

Next, the authors reveal the mechanics of this coupling. To this end, the authors search how the chip flows out of a workpiece and illustrate this manner in Figs. 4. 7(a) to (d). Figs. 4. 7(a) to (d) show the results obtained under the same cutting speed as in Fig. 4. 5 and Fig. 4. 6 (V_0=75 m/min). Fig 4. 7(a) is for an instant when the chip begins to flow out, Fig. 4. 7(b) for an instant when chatter vibration occurs at the point B, Fig. 4. 7(c) for an instant when this chatter ceases, Fig. 4. 7(d) for an instant when the depth of cut has been thicker than that in Fig. 4. 7(c). Normal stress σ and shearing stress τ, which exert on the cuttig edge, are also shown in Fig. 4. 7(b).[30] Here, the ratio of the chip thickness to the depth of cut t_c/d and the ratio of the contact length of the chip with a tool on the rake face to the depth of cut l_c/d are found in the same method as explained in the previous chapter. These ratios are constant for the various feed rates and the various depth of cut. Table 4. 2 shows these ratios for various cutting speeds and also for the experiments conducted in the Chapter 3. Considering Fig. 4. 7(b), the authors can describe the mechanics of this coupling as follows.

(1) Imagine the case that a workpiece is disturbed to move downward before the chip flows out along the rake face ($\dot{y}<0$).

(2) At this time the chip is pressed on the rake face and begins to flow out along this face.

(3) This action increases the magnitude of shearing stress ($-\tau$) on the rake face.

(4) The increase of the shearing stress increases the horizontal cutting force F_x and moves a workpiece to the right direction.

(5) A motion of a workpiece to the right direction decreases the depth of cut and then decreases the horizontal and the vertical cutting forces F_x, F_y.

(6) When a workpiece is disturbed to move upward ($\dot{y}>0$), the shearing force decreases and finally the increase of the vertical cutting force makes a workpiece move upward more.

Table 4. 2. Effect of cutting speed on ratios, t_c/d and l_c/d

Tool	Chapter 4			Chapter 3
V_0 (m/min)	50	75	100	50, 75
tc/d	6. 2	4. 4	3. 3	2. 5
lc/d	6. 2	5. 6	5. 1	5. 0

These descriptions indicate that chatter is self-excited by the motion of the chip on the rake face. The authors have already explained that this motion looks like the stick-slip motion. This particular motion, however, doesn't occur in the depth of cut illustrated by Fig. 4. 7(d) because in the case of Fig. 4. 7(d) the chip flows out smoothly along the rake face. In other words, chatter occurs in a limited range of the depth of cut. To confirm

this character, the authors hit a workpiece with a hammer at the depth of cut illustrated by Fig. 4. 7(d) and found out that the vibration died out after a short time.

Finally, the authors estimated the amplitude of the chatter vibrations. Forgoing consideration indicates us that the amplitude of the chatter depends on a time that the cutting edge passes through an unstable range of the depth of cut. Fig. 4. 8 shows the maximum amplitudes of chatter x_{max}, y_{max} versus the instantaneous feed rate $\dot{d}$. In Fig. 4. 8 the solid-line curves present rectangular hyperbola $y_{max}\dot{d}$=constant and $x_{max}\ \dot{d}$=constant. Further, for each cutting speed these curves agree well with the experimental results. This fact verifies the above implication.

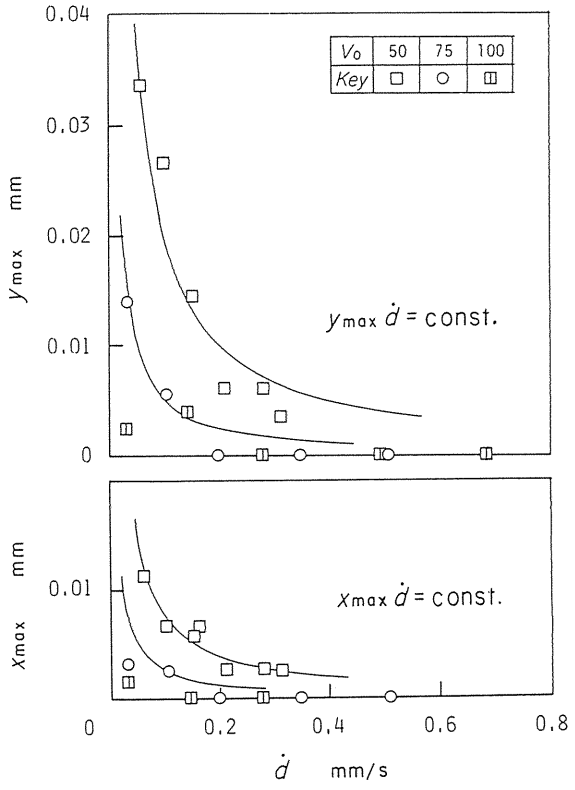

Fig. 4. 8. Relation between chatter amplitudes and instantaneous feed rate

Although this may be true, both x_{max} and y_{max} depend on the cutting speed. Table 4. 2 shows larger values of both the ratio t_c/d and l_c/d for smaller cutting speed. This property implies that the slower the cutting speed becomes the deeper becomes the depth of cut at which the chip flows out smoothly along the rake face.

Chapter 5. Effects of the Cutting Edge on the Chatter Vibration of a Workpiece when a Workpiece Partly Leaves a Tool[34)]

5. 1. *Introduction*

In the study of chatter, the illustration of a stability chart and the description of chatter are important subjects. Previous works[19,26)] on the description of chatter which made a workpiece partly leave a tool revealed the following characters of this chatter.

(1) Multi-regeneration effect took place and reduced an amplitude of chatter.[19)]

(2) When a workpiece was exposed to a large disturbance to leave a cutting edge, the workpiece commerced to chatter because of the non-linearity of the cutting forces.[26)]

In these works, however, there lack following considerations.

(1) What character does the chatter vibration show before it has fully developed?

(2) What effect does the cutting edge give on the chatter vibration when a workpiece partly leaves a tool?

Indeed, we often observe that a workpiece commerces to chatter soon after the cutting operation has begun and that a workpiece tends to partly leave a tool in finishing or at an initial stage of cutting operation. These observations confirm the striking effect of the cutting edge of a tool on chatter. The main subject of this chapter is the description of chatter, especially the description of the effect of the cutting edge on the cutting operation when a tool partly leaves a workpiece.[34)]

5. 2. *Experimental procedure*

The experimental procedure adopted in the present chapter is virtually the same as that fully described in the Chapter 2 so that only a brief description of the method is given here.

The steel shaft carrying a workpiece was held by a chuck at one end. To look into the effect of the stiffness of a workpiece, this shaft was either free at the other end (Condition 1) or simply supported by the tailstock (Condition 2). Under the Condition 1 the natural frequency of a workpiece was 111 Hz, and under the Condition 2 it was 243 Hz. Other vibratory parameters were already shown in Table 2. 1. Except a special case, the authors made experiments under the Condition 1. Further, the authors used two tools, i.e., tool I with a negative rake angle ($-5°$) and tool II with a positive rake angle ($10°$). Details are described in Table 2. 2.

5. 3. *Experimental results and its consideration*

In the Chapters 3 and 4, when cutting a rigid workpiece the authors described that both the cutting edge and the rake angle had a significant effect on chatter. This effect may be more significant in the case of cutting a slender workpiece.

First of all, the authors research what effect the configuration of a tool has in cutting a slender workpiece. Figs. 5. 1(a) and (b) show how the horizontal deflection x, the vertical deflection y, the horizontal cutting force F_x, the vertical cutting force F_y and the depth of cut d vary during 500 ms. Here, Figs. 5. 1(a) is for the tool I and Fig. 5. 1(b) is for the tool II. Marks ∇ have the same meaning denoted in the previous chapters. The comparison of Figs. 5. 1(a) and (b) shows us the following characters.

(1) Little difference lies between Figs. 5. 1(a) and (b), in other words, between two tools I, II.

With respect to the deflection, each of the differences between their magnitudes, their variations and their waves is little from $t=0$ ms to $t=450$ ms. The cutting force also shows

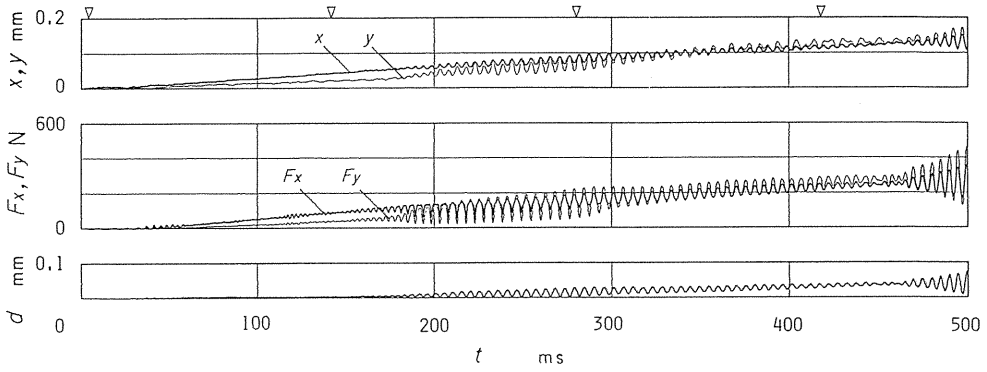

(a) Tool I

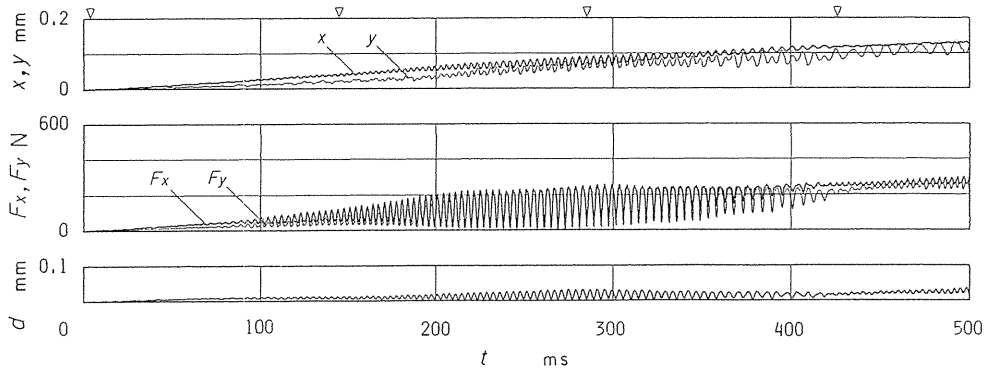

(b) Tool II

Fig. 5. 1. Example of chatter vibration (Condition 1, d_0=0.1 mm/rev, V_0=100 m/min)

the similar property. The chip which was produced in an initial stage of the cutting operation had the crescent-shape of length 2 mm in the both cases, tool I and II.

(2) The properties of chatter change as time goes on.

The chatter vibration appears in Figs. 5. 1(a) and (b) from the instant when the depth of cut is nearly zero. However, after t=300 ms, the variation of the cutting forces and the amplitude of the vibrations decrease as time goes on. Further, after t=300 ms, the cutting forces change its shape as time goes on.

These characters have not yet been reported by the authors or many other investigators. In the present chapter, the authors reveal the physical causes of these characters and describe the relation between the causes of these characters and the configuration of tools.

5. 3. 1. On little difference between tools I and II

The authors disclose the physical causes of little difference in this chapter. First, the authors show the static property of the cutting forces. Fig. 5. 2(a) illustrates the relation

between cutting forces and the depth of cut for the tool I and Fig. 5. 2(b) illustrates the similar relation for the tool II. Further, Table 5. 1 represents the ratio of a finite difference of cutting force to a finite difference of d, $\Delta F_x/\Delta d$ and $\Delta F_y/\Delta d$ for the cutting speed of 100 m/min and the depth of cut from d=50 to d=100 μm.

Now using this table, let's find out the relation of the static property of the cutting forces to the property of chatter. According to the previous works,[10,12] the stability chart and the build-up of chatter depend on the static property of cutting forces, especially the ratio $\Delta F_x/\Delta d$. Table 5. 1 represents that the value of $\Delta F_x/\Delta d$ for the tool I is different from that for the tool II. In spite of this fact, there lies little difference between Figs. 5. 1(a) and (b). In other words, we couldn't explain such little difference from the static property of the cutting forces.

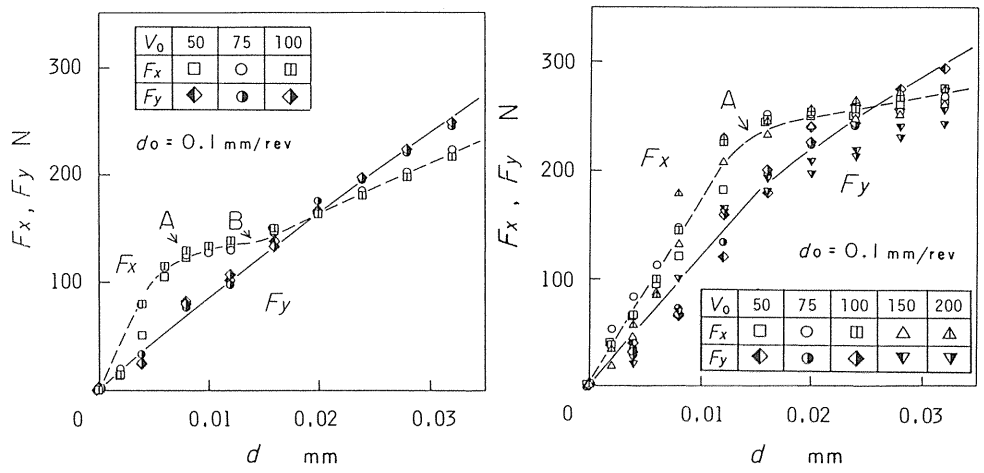

(a) Tool I (b) Tool II

Fig. 5. 2. Effect of depth of cut on static cutting forces

Table 5. 1. Static property of cutting force
(V_0=100 m/min, d=50~100 μm)

Tool	I	II
$\Delta F_x/\Delta d$ (MN/m)	2. 7	1. 1
$\Delta F_y/\Delta d$ (MN/m)	5. 0	3. 6

Then, the authors planed to describe the dynamic property of the cutting forces. Fig. 5. 3(a) illustrates the dynamic cutting forces F_x, F_y versus the depth of cut over a time of t=200 ms to t=205 ms for Fig. 5. 1(a). Fig. 5. 3(b) illustrates the similar relation over a time of t=300 ms to t=303.5 ms for Fig. 5. 1(b). In Figs. 5. 3(a) and (b), the dotted-lines show the static cutting forces (see Fig. 5. 2) and the solid lines show the dynamic cutting

forces. We find out commonly the following properties from Figs. 5. 3(a) and (b).
(1) In spite of its nonlinearity, the dynamic cutting forces have almost the same value as the static cutting forces. Tobias[26] also reported this character.
(2) The dynamic cutting forces change near the point at which the cutting operation starts[28] (see point A in Figs. 5. 2(a), (b)) over a range in which the ratios $\Delta F_x/\Delta d$ for the tool I and II have the same value. In other words, the dynamic cutting forces illustrated in Fig. 5. 3(a) seem to be like the dynamic cutting forces illustrated in Fig. 5. 3(b).

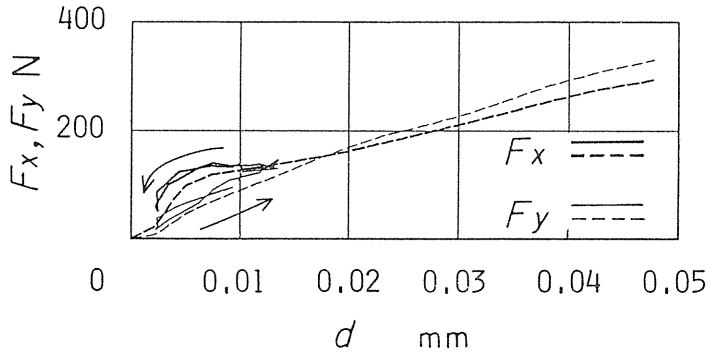

(a) Tool I

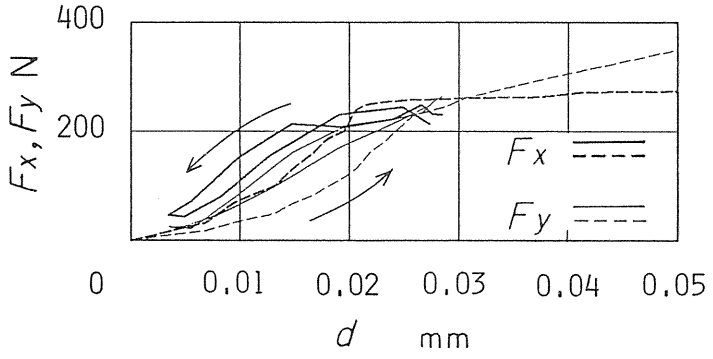

(b) Tool II

Fig. 5. 3. Effect of depth of cut on dynamic cutting forces
(Condition 1, d_0=0.1 mm/rev, V_0=100 m/min)

Above mentioned character (2) shows that little difference comes from the similarity of the dynamic cutting forces near the point A at which the cutting operation starts. Further, this character implies that the chatter, which the authors consider in this chapter, doesn't depend on the rake angle but depends only on the radius of the cutting edge.

5. 3. 2. On the variation of the properties of chatter

Now, the authors describe the characters of the variation in detail. They deal with the tool II because the properties of chatter are same for both tools I and II.

For the dynamic cutting forces F_x, F_y have a striking effect on chatter, especially its appearance and disappearance, the time variation of the dynamic cutting forces is shown in Figs. 5. 4(a) to (d). These figures teach us the following characters.

(1) When the chatter vibration grows (as illustrated by Figs. 5. 4(a) and (b)), the phase lag of the horizontal cutting force F_y behind the depth of cut d appears and it supplies an

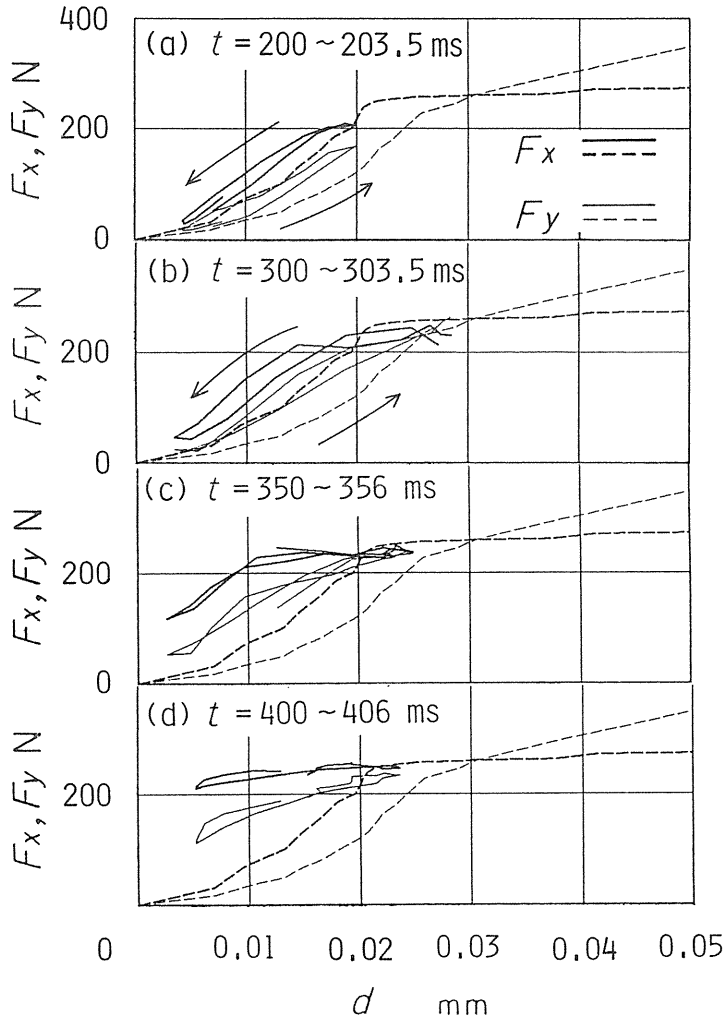

Fig. 5. 4. Time variation of dynamic cutting force (Condition 1, Tool II, d_0=0.1 mm/rev, V_0=100 m/min)

energy into the system in the range of the depth of cut from $d=0$ to the depth of cut at which the cutting operation starts.
(2) When chatter decreases its amplitude (see Figs. 5. 4(c) and (d)), the phase lag disappears and the supplement of the energy into the system ceases.
(3) The dynamic cutting forces illustrated in Fig. 5. 4(b) or (c) are the non-linear function regarding d. Deformed sinusoidal waves of the cutting forces in Fig. 5. 1(b) also depicted this non-linearity.
(4) Above the depth of cut at which the cutting operation starts, the dynamic cutting forces change linearly regarding d. This character is obvious in Fig. 5. 4(d).

Above four characters indicate that the ratio of the horizontal cutting force to the instantaneous feed rate[12] varies as a function of d and that the non-linearity of the cutting forces changes their shapes.

5. 3. 3. On the causes of chatter

Both kinds of chatter vibrations as reported in Chapters 3 and 4 have the following two characters.
(1) The chatter viabration occurs at the depth of cut where the chip flows out with fluctuation.
(2) The chatter vibration occurs in a limited range of the depth of cut.

The chatter vibration considered in this chapter doesn't show these characters, so we must find out another physical causes of chatter. In Chapters 3 and 4, the authors related the fashion of the chip flowing out both to the cutting forces and to the vibrations of a workpiece, and then revealed the physical causes of chatter. In this chapter, however, because the chip is broken into pieces by chatter, the authors can't apply the same method as used in Chapters 3 or 4 to find out the causes of chatter. Therefore, to find out the causes of chatter the authors related the deformation of chip to the variation of both the cutting forces and the deflections of a workpiece.[35]

First, a workpiece was simply supported by the tailstock (Condition 2). Then it was hit with a hammer and a deformed chip was got. Fig. 5. 5(a) illustrates the relation between the dynamic cutting forces and the depth of cut when a workpiece is hit at the depth of cut of $8\,\mu$m. Fig. 5. 5(b) shows the similar relation when a workpiece is hit at a depth of cut of $50\,\mu$m. The abscissa of Fig. 5. 5(b) is enlarged to a scale of twice the abscissa of Fig. 5. 5(a). Comparing Fig. 5. 5(a) with Fig. 5. 4(a) and also Fig. 5. 5(b) with Fig. 5. 4(b) indicate that the dynamic cutting forces don't depend on the stiffness of a workpiece. In other words, Fig. 5. 5.(a) gives the same experimental result as Fig. 5. 4(a) and also Fig. 5. 5(b) gives the same result as Fig. 5. 4(b).

Fig. 5. 6(a) is a photomicrograph of produced chip in relation to Fig. 5. 5(a), and Fig. 5. 6(b) is a similar photomicrograph in relation to Fig. 5. 5(b). Instants denoted by Numbers ① to ⑤ in Figs. 5. 5(a) and (b) coincide with instants denoted by Numbers ① to ⑤ in Figs. 5. 7(a) and (b).

We can find out the following characters from Figs. 5. 5(a), (b), Figs. 5. 6(a) and (b).
(1) In spite of the variations of the depth of cut from $d=8\,\mu$m to $d=24\,\mu$m, a thickness of produced chip is constant. (This phenomenon occurs at the point denoted by Number ①.)
(2) A thickness of chip t_c equals to $50\,\mu$m at the depth of cut of $d=0$. (at the point ②) the difference of the depth of cut.
(4) Shear angle varies significantly both from the instant denoted by ① to the instant ②, and from the instant ② to the instant ③.

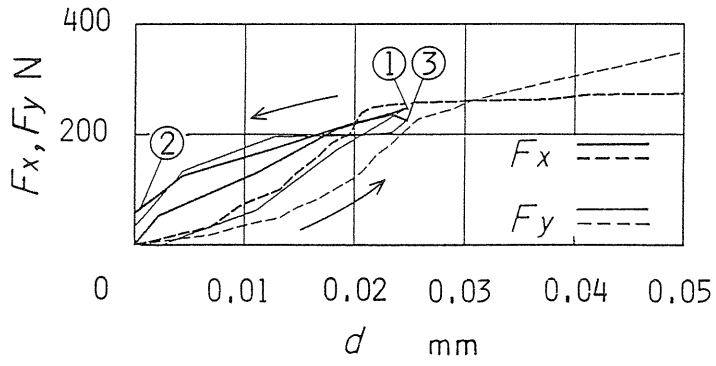

(a) Disturbed at depth of cut of 8 μm

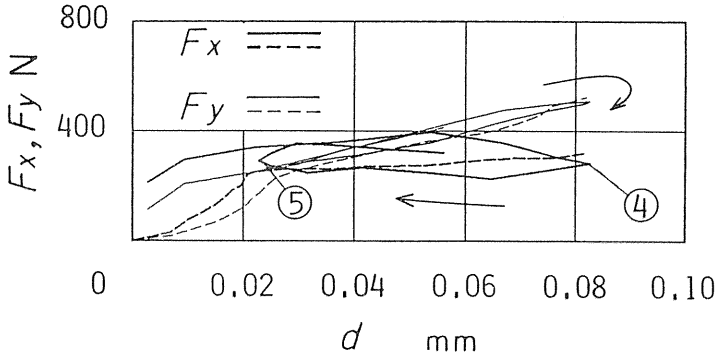

(b) Disturbed at depth of cut of 50 μm

Fig. 5. 5. Example of vibration caused by horizontal disturbance (Condition 2, Tool II, d_0=0.05 mm/rev, V_0=75 m/min)

(5) The ratios of the thickness of chip to the depth of cut at the instant ④ or ⑤ have the same value (t_c/d=3.0).
(6) Shear angle varies slightly from the instant ④ to ⑤.
(7) Fig. 5. 6(a) shows that the ratio of the thickness of chip to the same depth of cut is different from one shown in Fig. 5. 6(b). The ratio t_c/d equals 5.0 at the instant ③ when the depth of cut is 24 μm. On the contrary, the ratio t_c/d equals 3.0 at the instant ⑤ when the depth of cut is 23 μm.

Above mentioned experimental results tell us the physical causes of chatter as follows.
(1) Before the cutting operation starts (Fig. 5. 5(a) and Fig. 5. 6(a)). The chip flows out in a formation illustrated by Fig. 5. 7. At this state, when hitting a workpiece in the horizontal direction, the depth of cut increases. At the same time an angle ψ at which the chip flows out increases and the shear angle decreases. Although the increase of the depth of cut enlarges the thickness of produced chip, the decrease of shear angle reduces the thickness of produced chip. These two types of character cancel to one another and

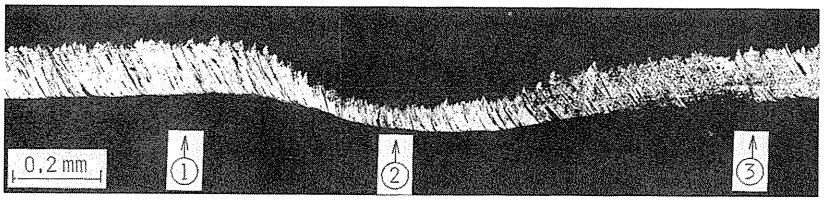

(a) Disturbed at depth of cut of 8 μm

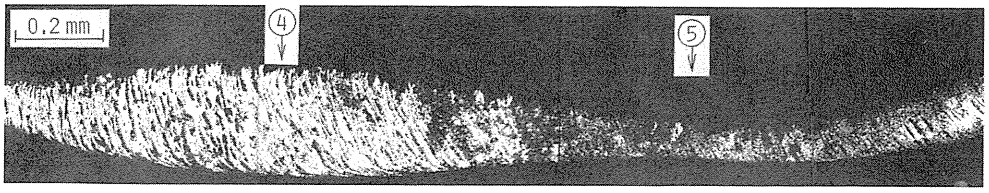

(b) Disturbed at depth of cut of 50 μm

Fig. 5. 6. Photomicrograph of generated chip (Condition 2, Tool II, d_0=0.05 mm/rev, V_0=75 m/min)
The bottom of these chips is rubbing the cutting edge and moving to the left

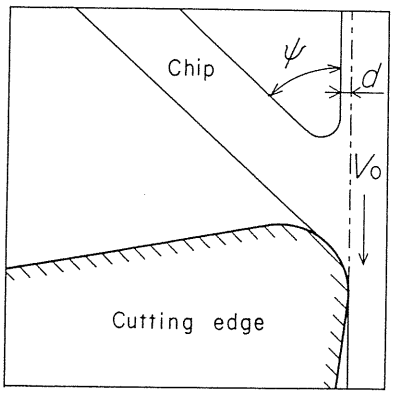

Fig. 5. 7. Flow pattern of generated chip (Tool II)

keep the thickness of chip nearly constant. The shear angle, however, strikingly vary as shown in Fig. 5. 6(a). Further, this phenomenon makes the cutting forces lag and causes the chatter vibration.

(2) After the cutting operation starts (Fig. 5. 5(b) and Fig. 5. 6(b)). Above-mentioned characters (5) and (6) are the same ones that Pearce has already reported.[35] According to his report, dynamic cutting forces at this instant depend on the interaction between the

rake face and the produced chip. Also his report indicates that the dynamic cutting forces illustrated in Fig. 5. 5(b) act as damping forces because of a small velocity of vibration and that this property of dynamic cutting forces makes chatter die out.

Finally, the authors estimate the ratio of the horizontal cutting force to the instantaneous feed rate with respect to Fig. 5. 5(a). Let the horizontal cutting force F_x be a function both of the depth of cut d and of the horizontal velocity of a workpiece $\dot{x}$. During a short time, the relations can be expressed by

$$d = a_0 - x$$

$$F_x(d,\ x) = b_0 - k_c x + c_d \dot{x}$$

where all parameters a_0, b_0, k_c and c_d are constant ($k_c>0$, $c_d>0$) and the term $c_d\dot{x}$ gives a negative damping to a system. Now, making the definite integral from $t=0$ to $t=T$, we can estimate the negative damping factor c_d as follows;

$$\int_0^T F_x \dot{x}\ dt = \int_0^T (b_0 - k_c x + c_d \dot{x}\ )\dot{x}\ dt = c_d \int_0^T \dot{x}^2 dt$$

$$c_d = \frac{\int_0^T F_x \dot{x}\ dt}{\int_0^T \dot{x}^2 dt}$$

Numerical calculation of Fig. 5. 5(a) tells us that c_d equals 260 Ns/m. The estimation of the average value of damping factors of a workpiece c with respect to Table 2. 1 gives us following values.

Fixed-free condition 1 (without the tailstock)	$c=75$ Ns/m
Fixed-simply supported condition 2 (with the tailstock)	$c=700$ Ns/m

Accordingly, the negative damping factor c_d caused by cutting operation is larger than c, the damping of a workpiece without the tailstock and then c_d causes the chatter vibration.

Conclusions

In this paper, chatter vibrations which occurred soon after a cutting operation had begun were researched experimentally. First, the authors observed the built-up of chatter during the first and subsequent revolutions of the workpiece following the beginning of the cutting operation. This observation showed a good agreement with the theoretical results. Next, the primary chatter was researched. It was found that the configuration of a tool and the depth of cut had significant effects on the occurrence of chatter. There existed two instability regions regarding the depth of cut. The first instability region had a close connection with the roundness of the cutting edge and the second one did with the rake angle of the tool. These experimental results confirmed an empirical results that the chatter was most apt to occur when a blunt tool or a tool with a large negative rake angle was used. Finally, characters of chatter were researched when cutting a slender workpiece,

i.e. a workpiece with insufficient rigidity. In this case, only the roundness of the cutting edge affected the chatter vibration. Deformation of the chip in the vicinity of the cutting edge caused a time lag of the horizontal cutting force and then yielded the chatter.

Acknowledgment

We would like to express our appreciation to Messrs. H. Nomura, Y. Goto, and T. Shiratsuchi for their help with the experiments, and to Mr. N. Yamaguchi for his assistance in preparing the experimental apparatus.

References

1) Arnold, R.N., "The Mechanism of the Tool Vibration in the Cutting of Steel", Proceedings of the Institution of Mechanical Engineers, Vol. 154 (1946), pp. 261–276.
2) Hahn, R.S., "Metal-Cutting Chatter and Its Elimination", Trans. ASME, Vol. 75, No. 6 (Aug. 1953), pp. 1073–1080.
3) Doi, S., "On the Chatter Vibrations of Lathe Tools", Memoirs of the Faculty of Engineering, Nagoya Univ. Vol. 5, No. 2 (Oct. 1953), pp. 179–216.
4) Doi, S., Simoyama, Y. and Kuroda, J., "On Chatter vibration due to Main Spindle of a Lathe", Jour. Jpn. Soc. Mech. Eng., (in Japanese), Vol. 54, No. 385 (Feb. 1951), pp. 39–44.
5) Doi, S. and Kato, S., "On Chatter Vibration due to flexible Lathe Tool", Trans. Jpn. Soc. Mech. Eng., (in Japanese), Vol. 19, No. 86 (Oct. 1953), pp. 28–34.
6) Doi, S. and Kuroda, J., "On Chatter vibration due to Main Spindle of a Lathe (2nd Report)", Trans. Jpn. Soc. Mech. Eng., (in Japanese), Vol. 19, No. 86 (Oct. 1953), pp. 34–39.
7) Doi, S. and Kato, S. "On Chatter vibration due to Main Spindle of a Lathe (3rd Report)", Trans. Jpn. Soc. Mech. Eng., (in Japanese), Vol. 20, No. 90 (Feb. 1954), pp. 61–65.
8) Doi, S. and Kato, S. "On Chatter vibration due to Main Spindle of a Lathe (5th Report)", Trans. Jpn. Soc. Mech. Eng., (in Japanese), Vol. 21, No. 110 (Oct. 1955), pp. 727–731.
9) Doi, S. et. al. "On Chatter vibration due to Main Spindle of a Lathe (6th Report)", Trans. Jpn. Soc. Mech. Eng., (in Japanese), Vol. 22, No. 118 (June 1956), pp. 408–411.
10) Kato, S., "Theoretical Research on Chatter Vibration of Lathe Tools", Memoirs of the Faculty of Engineering, Nagoya Univ. Vol. 10, No. 2 (Oct. 1958), pp. 117–174.
11) Albrecht, P., "Self-Induced Vibrations in Metal Cutting", Trans. ASME, Ser. B, Vol. 84, No. 4 (Nov. 1962), pp. 405–417.
12) Tobias, S.A. and Fishwick, W., "The Chatter Vibration of the Lathe Tools under Orthogonal Cutting Condition", Trans. ASME, Vol. 80, No. 5 (July 1958), pp. 1079–1088.
13) Doi, S. and Kato, S. "On Chatter vibration due to Main Spindle of a Lathe (4th Report)", Trans. Jpn. Soc. Mech. Eng., (in Japanese), Vol. 21, No. 102 (Feb. 1955), pp. 110–113.
14) Kato, S., "On the Theoretical Research of Chatter Vibration (1st Report)", Trans. Jpn. Soc. Mech. Eng., (in Japanese), Vol. 24, No. 138 (Feb. 1958), pp. 115–119.
15) Kato, S. and Goshima, T., "On the Theoretical Research of Chatter Vibration (2nd Report)", Trans. Jpn. Soc. Mech. Eng., (in Japanese), Vol. 24, No. 138 (Feb. 1958), pp. 119–124.
16) Ota, H. and Kono, K., "Chatter Vibrations of Machine Tool or Work with Directional Stiffness Inequality", Bull. JSME, Vol. 16, No. 96 (June 1973), pp. 947–954.
17) Ota, H. and Kono, K., "On Chatter Vibrations of Machine Tool or Work Due to Regenerative Effect and Time Lag", Trans. ASME, Ser. B, Vol. 96, No. 4 (Nov. 1974), pp. 1337–1346.
18) Ota, H. and Kono, K., "On the Regenerative Chatter Vibrations of Machine Tool or Work", Research Report of the Faculty of Engineering, Tokushima Univ., (in Japanese), No. 20 (March, 1975), pp. 73–83.

19) Kondo, S. et. al., "Self-excited Vibration in Turning and Generated Chatter Mark", Trans. Jpn. Soc. Mec. Eng., (in Japanese), Vol. 46, No. 409, C (Sept. 1980), pp. 1024–1032.
20) Kaneko, T. et. al., "Behaviour of the Self-excited Vibration Considering Multiple Regeneration Effect", Trans. Jpn. Soc. Mec. Eng., (in Japanese), Vol. 50, No. 454, C (June 1984), pp. 961—969.
21) Ota, H., Mizutani, K. and Kawai, T., "On the Occurrence of Regenerative Chatter Vibrations", Trans. Jpn. Soc. Mech. Eng., (in Japanese), Vol. 52, No. 480, C (Aug. 1986), pp. 2278–2286.
22) Ota, H., Mizutani, K. and Kawai, T., "On the Occurrence of Regenerative Chatter Vibrations", JSME Int. J. Vol. 30, No. 262 (April 1987), pp. 661–669.
23) Doi, M., Masuko, M. and Ito, Y., Trans. Jpn. Soc. Mech. Eng., (in Japanese), Vol. 48, No. 429 (May 1982), pp. 761—768.
24) Albrecht, P., "New Developments in the Theory of the Metal-Cutting Process, The Ploughing Process in Metal Cutting", Trans. ASME, Ser B, Vol. 82, No. 4 (Nov. 1960), pp. 348–358.
25) Hook, C.J. and Tobias, S.A., "Finite Amplitude Instability–A New Type of Chatter", Proc. 4th Int. M.T.D.R., Conf. (Sep. 1963), pp. 97–100.
26) Shi, E.M. and Tobias, S.A., "Theory of Finite Amplitude Machine Tool Instability", Int. J. M.T.D.R., Vol. 24, No. 1 (Feb. 1984), pp. 45–69.
27) Yuta, T., "Fundamental Studies on the Beginning Phenomena of Cutting (1st Report)", Jour. Jpn. Prec. Eng., (in Japanese), Vol. 35, No. 5 (1969), pp. 292–298.
28) Yamamoto, A. and Nakamura, S., "Study on the Rubbing-Cutting Transition Phenomena at the Depth of Cut Increse Gradually", Jour. Jpn. Prec. Eng., (in Japanese), Vol. 34, No. 5 (1968), pp. 310–315.
29) Yamamoto, A. and Nakamura, S., "Study on the Rubbing-Cutting Transition Phenomena at the Depth of Cut Increse Gradually (2nd Report)", Jour. Jpn. Prec. Eng., (in Japanese), Vol. 35, No. 3 (1969), pp. 164—168.
30) Yamamoto, A. and Nakamura, S., "Study on the Rubbing-Cutting Transition Phenomena with the Gradually Incresing Depth of Cut (3rd Report)", Jour, Jpn. Prec. Eng., (in Japanese), Vol. 36, No. 3 (1970), pp. 176–182.
31) Ota, H., Mizutani, K. and Kawai, T., "Effects of the Cutting Edge on the Chatter Vibrations of a Workpiece (1st Report, Case of Positive Rake Angle)", Trans. Jpn. Soc. Mech. Eng., (in Japanese), Vol. 54, No. 500, C (April 1988), pp. 968–975.
32) Kita, Y., Ido, M. and Kawasaki, N., "A Study of the Cutting Mechanism with Large Negative Rake Angle", Jour. Jpn. Prec. Eng., (in Japanese), Vol. 44, No. 9 (Sept. 1978), pp. 1099—1104.
33) Ota, H., Mizutani, K., Kawai, T. and Goto, Y., "Effects of the Cutting Edge on the Chatter Vibrations of a Workpiece (2nd Report, Case of Negative Rake Angle)", Trans. Jpn. Soc. Mech. Eng., (in Japanese), Vol. 54, No. 504, C (Aug. 1988), pp, 1961–1966.
34) Ota, H., Mizutani, K., Kawai, T. and Shiratsuchi, T., "Effects of the Cutting Edge on the Chatter Vibrations of a Workpiece (3rd Report, The Case that a Workpiece partly leaves a Tool)", Trans. Jpn. Soc. Mech. Eng., (in Japanese), Vol. 54, No. 504, C (Aug. 1988), pp. 1967–1973.
35) Pearce, D.F. and MacManus, B.R., "Dynamic Chip Formation and its Significance to Machining Stability", Proc. Inst. Mech. Engineers, Vol. 187, No. 21 (1973), pp. 273–283.
36) Ota, H., Kondo, E. and Yamada, T., "Regenerative Chatter Vibrations of Turning Workpiece (1st Report, Two Degrees of Freedom and its Stability Criterion)," Trans. Jpn. Soc. Mech. Eng., (in Japanese), Vol. 54 No. 504, C (Aug. 1988), pp. 1953–1960.